

1 Event History Analysis for psychological time-to-event data: A tutorial in R with examples
2 in Bayesian and frequentist workflows

3 Sven Panis¹ & Richard Ramsey¹

4 ¹ ETH Zürich

5 Author Note

6 Neural Control of Movement lab, Department of Health Sciences and Technology
7 (D-HEST). Social Brain Sciences lab, Department of Humanities, Social and Political
8 Sciences (D-GESS).

9 The authors made the following contributions. Sven Panis: Conceptualization,
10 Writing - Original Draft Preparation, Writing - Review & Editing; Richard Ramsey:
11 Conceptualization, Writing - Review & Editing, Supervision.

12 Correspondence concerning this article should be addressed to Sven Panis, ETH
13 GLC, room G16.2, Gloriustrasse 37/39, 8006 Zürich. E-mail: sven.panis@hest.ethz.ch

14

Abstract

15 Time-to-event data such as response times and saccade latencies form a cornerstone of
16 experimental psychology, and have had a widespread impact on our understanding of
17 human cognition. However, the orthodox method for analysing such data – comparing
18 means between conditions – is known to conceal valuable information about the timeline of
19 psychological effects, such as their onset time and duration. The ability to reveal
20 finer-grained, “temporal states” of cognitive processes can have important consequences for
21 theory development by qualitatively changing the key inferences that are drawn from
22 psychological data. Luckily, well-established analytical approaches, such as event history
23 analysis (EHA), are able to evaluate the detailed shape of time-to-event distributions, and
24 thus characterise the time course of psychological states. One barrier to wider use of EHA,
25 however, is that the analytical workflow is typically more time-consuming and complex
26 than orthodox approaches. To help achieve broader uptake of EHA, in this paper we
27 outline a set of tutorials that detail one distributional method known as discrete-time
28 EHA. We touch upon several key aspects of the workflow, such as how to process raw data
29 and specify regression models, and we also consider the implications for experimental
30 design, as well as how to manage inter-individual differences. We finish the article by
31 considering the benefits of the approach for understanding psychological states, as well as
32 the limitations and future directions of this work. Finally, the project is written in R and
33 freely available, which means the approach can easily be adapted to other data sets.

34 *Keywords:* response times, event history analysis, Bayesian multilevel regression
35 models, experimental psychology, cognitive psychology

36 Word count: 13574

37

1. Introduction

38 1.1 Motivation and background context: Comparing means versus 39 distributional shapes

40 In experimental psychology, it is standard practice to analyse response times (RTs),
41 saccade latencies, and fixation durations by calculating average performance across a series
42 of trials. Such mean-average comparisons have been the workhorse of experimental
43 psychology over the last century, and have had a substantial impact on theory development
44 as well as our understanding of the structure of cognition and brain function. However,
45 differences in mean RT conceal important pieces of information, such as when an
46 experimental effect starts, how long it lasts, how it evolves with increasing waiting time,
47 and whether its onset is time-locked to other events (Panis, 2020; Panis, Moran,
48 Wolkersdorfer, & Schmidt, 2020; Panis & Schmidt, 2016, 2022; Panis, Torfs, Gillebert,
49 Wagemans, & Humphreys, 2017; Panis & Wagemans, 2009; Wolkersdorfer, Panis, &
50 Schmidt, 2020). Such information is useful not only for the interpretation of experimental
51 effects under investigation, but also for cognitive psychophysiology and computational
52 model selection (Panis, Schmidt, Wolkersdorfer, & Schmidt, 2020).

53 As a simple illustration, Figure 1 shows the results of several simulated RT data sets,
54 which show how mean-average comparisons between two conditions can conceal the shape
55 of the underlying RT distributions. For instance, in examples 1-3, mean RT is always
56 comparable between two conditions, while the distributions differ (Figure 1, left). In
57 contrast, in examples 4-6, mean RT is lower in condition 2 compared to condition 1, but
58 the RT distributions differ in each case (Figure 1, right). Therefore, a comparison of means
59 would lead to a similar conclusion in examples 1-3, as well as examples 4-6, whereas a
60 comparison of the distributions would lead to a different conclusion in every case.

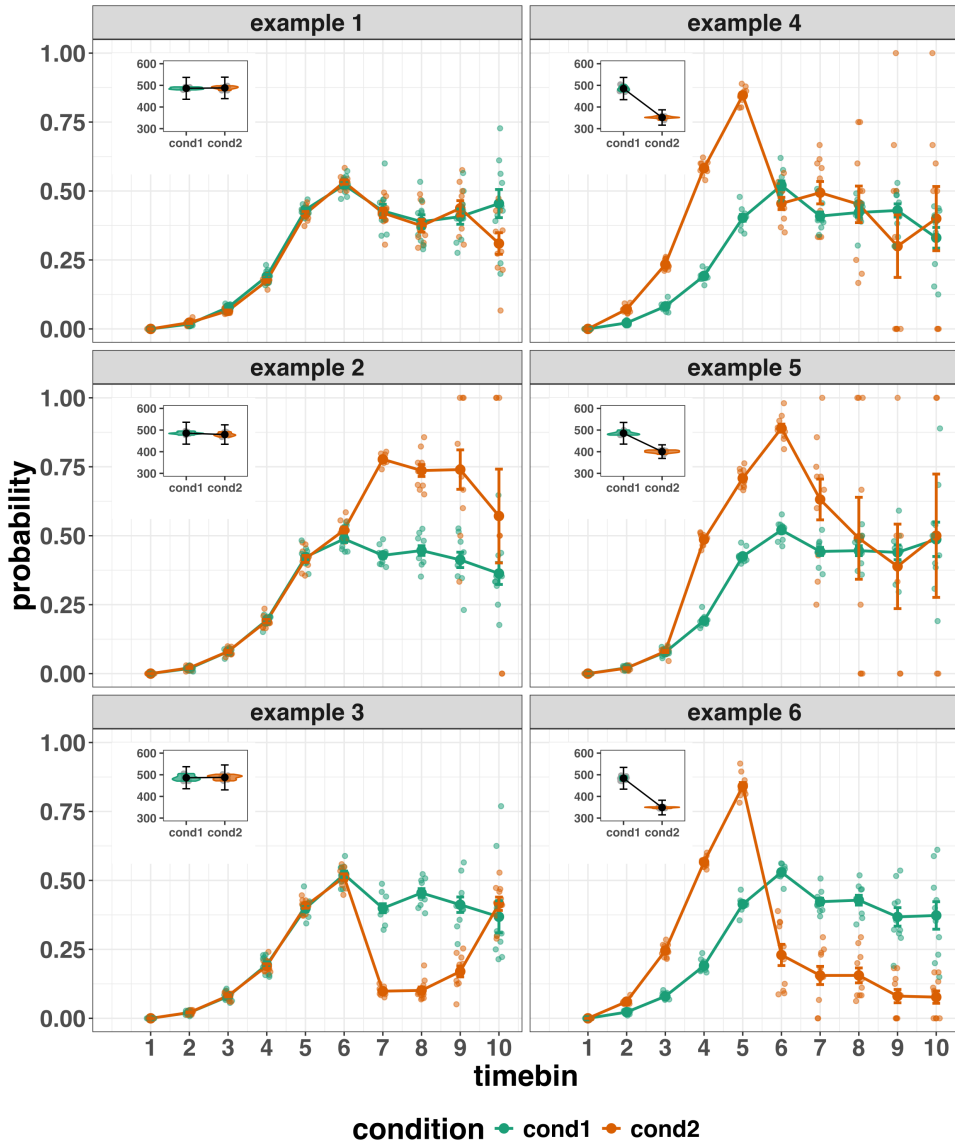


Figure 1. Means versus distributional shapes for six different simulated data set examples.

The first second after stimulus onset is divided in ten bins of 100 ms. Timebin indicates the bin rank. The first bin is (0,100], the last bin is (900,1000]. For our purposes here, it is enough to know that the distributions plotted represent the probability of an event occurring in that timebin, given that it has not yet occurred. Insets show mean response time per condition.

62 data across trials, a distributional approach offers the possibility to reveal the time course
63 of psychological states. As such, the approach permits different kinds of questions to be
64 asked, different inferences to be made, and it holds the potential to discriminate between
65 different theoretical accounts of psychological and/or brain-based processes. For example,
66 the distributions in example 4 show that the effect starts between 100 and 200 ms (in
67 timebin 2) and is gone when the waiting time reaches 500 ms or more. In contrast, in
68 example 5, the effect starts around 300 ms and is gone by 700 ms. And in example 6, the
69 effect reverses between 500 and 600 ms. What kind of theory or theories could account for
70 such effects? Are there new auxiliary assumptions that theories need to adopt? And are
71 there new experiments that need to be performed to test the novel predictions that follow
72 from these analyses? As we show later using published examples, for many psychological
73 questions, such “temporal states” information can be theoretically meaningful by leading to
74 more fine-grained understanding of psychological processes, as well as adding a relatively
75 under-used dimension – the passage of time – to the theory building toolkit.

76 From a historical perspective, it is worth noting that the development of analytical
77 tools that can estimate or predict whether and when events will occur is not a new
78 endeavour. Indeed, hundreds of years ago, analytical methods were developed to predict
79 the duration of time until people died (e.g., Halley, 1693; Makeham, 1860). The same logic
80 has been applied to psychological time-to-event data, as previously demonstrated (Panis,
81 Schmidt, et al., 2020).

82 1.2 Aims and structure of the paper

83 In this paper, we focus on a distributional method for time-to-event data known as
84 discrete-time Event History Analysis (EHA), a.k.a. survival analysis, hazard analysis,
85 duration analysis, failure-time analysis, and transition analysis (Singer & Willett, 2003).
86 We hope to show the added value of EHA for knowledge and theory building in cognitive
87 psychology and related areas of research, such as cognitive neuroscience. Most importantly,

88 we provide tutorials that provide step-by-step code and instructions in the hope that we
89 can enable others to use EHA in a more routine, efficient and effective manner.

90 We first provide a brief overview of EHA to orient the reader to the basic concepts
91 that we will use throughout the paper. However, this will remain relatively short, as this
92 has been covered in detail before (Allison, 1982, 2010; Singer & Willett, 2003). Indeed, our
93 primary aim here is to introduce the set of tutorials, which explain **how** to do such
94 analyses, rather than repeat in any detail **why** you may do them.

95 We provide seven different tutorials, which are written in the R programming
96 language and publicly available on our Github page ([https://github.com/sven-panis/
97 Tutorial_Event_History_Analysis](https://github.com/sven-panis/Tutorial_Event_History_Analysis)), along with all of the other code and material
98 associated with the project. The tutorials provide hands-on, concrete examples of key parts
99 of the analytical process, so that others can apply EHA to their own time-to-event data.
100 Each tutorial is provided as an RMarkdown file, so that others can download and adapt
101 the code to fit their own purposes. Additionally, each tutorial is made available as a .html
102 file, so that it can be viewed by any web browser, and thus available to those that do not
103 use R. Finally, the manuscript itself is written in R using the papaja package (Aust &
104 Barth, 2024), which makes it computationally reproducible, in terms of the underlying data
105 and figures.

106 In Tutorial 1a, we illustrate how to process or “wrangle” a previously published RT +
107 accuracy data set to calculate descriptive statistics when there is one independent variable.
108 The descriptive statistics are plotted, and we comment on their interpretation. In Tutorial
109 1b we provide a generalisation of this approach to illustrate how one can calculate the
110 descriptive statistics when using a more complex design, such as when there are two
111 independent variables.

112 In Tutorial 2a, we illustrate how one can fit Bayesian multilevel regression models to
113 RT data using the R package brms. We also perform prior predictive checks, compare

models, and interpret the plots of the predicted hazard functions for the selected model, and the posterior distributions of our contrasts of interest. In Tutorial 2b we fit Bayesian multilevel regression models to *timed* accuracy data to perform a micro-level speed-accuracy tradeoff (SAT) analysis, which complements the EHA of RT data for choice RT data.

In Tutorial 3a, we shortly illustrate how to fit similar multilevel regression models for RT data in a frequentist framework using the R package lme4. We then briefly compare and contrast these inferential frameworks when applied to EHA. In Tutorial 3b, we illustrate how to perform the SAT analysis in a frequentist framework.

In tutorial 4, we illustrate one approach to planning how much data to collect in an experiment using EHA. We use data simulation techniques to vary sample size and trial count per condition until a certain degree of statistical power or precision is reached.

In summary, even though EHA is a widely used statistical tool and there already exist many excellent reviews (e.g., Blossfeld & Rohwer, 2002; Box-Steffensmeier, 2004; Hosmer, Lemeshow, & May, 2011; Teachman, 1983) and tutorials (e.g., Allison, 2010; Landes, Engelhardt, & Pelletier, 2020) on its general use-cases, we are not aware of any tutorials that are aimed at psychological time-to-event data, and which provide worked examples of the key data processing and multilevel regression modelling steps. Therefore, our ultimate goal is twofold: first, we want to convince readers of the many benefits of using EHA when dealing with time-to-event data with a focus on psychological time-to-event data, and second, we want to provide a set of practical tutorials, which provide step-by-step instructions on how you actually perform a discrete-time EHA on time-to-event data such as RT data, as well as a complementary discrete-time SAT analysis on timed accuracy data.

137 **2. A brief introduction to event history analysis**

138 We recommend several excellent textbooks for a comprehensive background context

139 to EHA (Allison, 2010; Singer & Willett, 2003) and for a more general introduction to

140 understanding regression equations (Gelman, Hill, & Vehtari, 2020; Winter, 2019). Our

141 focus here is not on providing a detailed account of the underlying regression equations,

142 since this topic has been comprehensively covered many times before. Instead, we want to

143 provide an intuition regarding how EHA works in general, as well as in the context of

144 experimental psychology. As such, we only supply regression equations in section D of the

145 supplementary material.

146 **2.1 Basic features of event history analysis**

147 To apply EHA, one must be able to:

148 1. define an event of interest that represents a qualitative change that can be situated in

149 time (e.g., a button press, a saccade onset, a fixation offset, etc.);

150 2. define time point zero (e.g., target stimulus onset, fixation onset, etc.);

151 3. measure the passage of time between time point zero and event occurrence in discrete

152 or continuous time units.

153 In EHA, the definition of hazard and the type of models employed depend on

154 whether one is using continuous or discrete time units. Since our focus here is on hazard

155 models that use discrete time units, we describe that approach. After dividing time in

156 discrete, contiguous time bins indexed by t (e.g., $t = 1:10$ timebins), let RT be a discrete

157 random variable denoting the rank of the time bin in which a particular person's response

158 occurs in a particular experimental condition. For example, the first response might occur

159 at 546 ms and it would be in timebin 6 (any RTs from 501 ms to 600 ms).

160 Discrete-time EHA focuses on the discrete-time hazard function of event occurrence
161 and the discrete-time survivor function (Figure 2). The equations that define both of these
162 functions are reported in part A of the supplementary material. The discrete-time hazard
163 function gives you, for each time bin, the probability that the event occurs (sometime) in
164 bin t, given that the event does not occur in previous bins. In other words, it reflects the
165 instantaneous likelihood that the event occurs in the current bin, given that it has not yet
166 occurred in the past, i.e., in one of the prior bins. In contrast, the discrete-time survivor
167 function cumulates the bin-by-bin risks of event *nonoccurrence* to obtain the survival
168 probability, the probability that the event occurs after bin t. In other words, the survivor
169 function gives you for each time bin the likelihood that the event occurs in the future, i.e.,
170 in one of the subsequent timebins.

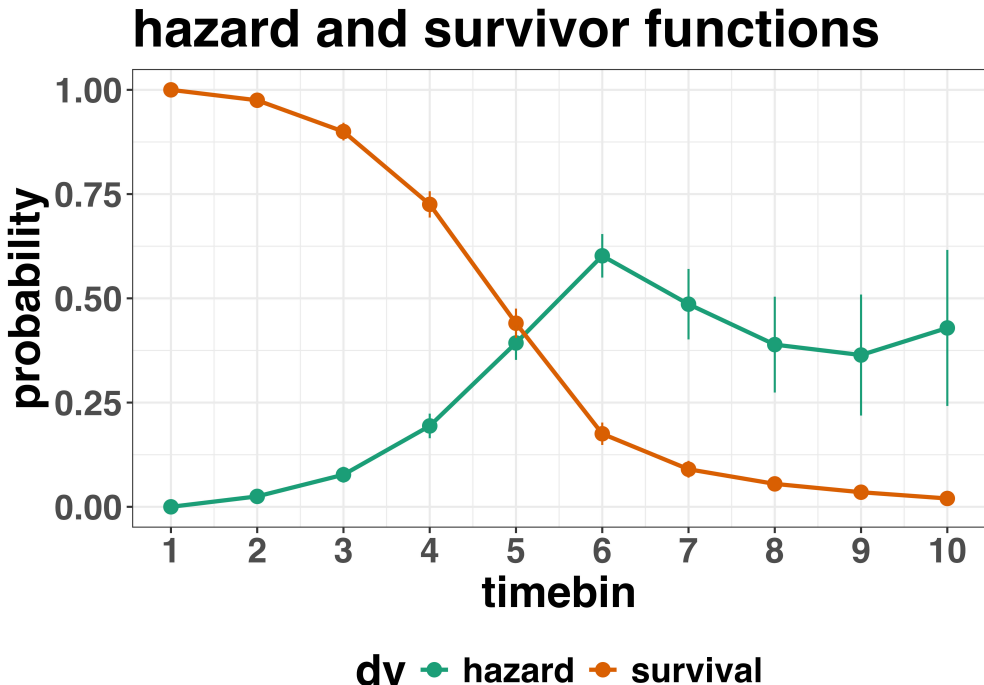


Figure 2. Discrete-time hazard and survivor functions. Discrete time-to-event data were simulated for 200 trials of 1 experimental condition. Error bars represent ± 1 standard error of the respective proportion. While the hazard function is the vehicle for inferring the time course of cognitive processes, the survival probability $S(t-1)$ can help to qualify or provide context to the interpretation of the hazard probability $h(t)$. For example, the high hazard of $.60 = h(t=6)$ is experienced only by 44 percent of the trials, as $S(t=5) = .44$. Because the survivor function is a decreasing function of time, the error bars in later parts of the hazard function will always be wider and less precise compared to earlier parts.

¹⁷¹ 2.2 Benefits of event history analysis

¹⁷² Statisticians and mathematical psychologists recommend focusing on the hazard
¹⁷³ function when analyzing time-to-event data for various reasons. We do not cover these
¹⁷⁴ benefits in detail here, as these are more general topics that have been covered elsewhere in
¹⁷⁵ textbooks. Instead, we briefly list the benefits below, and refer the reader to section F of
¹⁷⁶ the supplementary material for more detailed coverage of the benefits. The benefits include:

- 177 1. Hazard functions are more diagnostic than density functions when one is interested in
178 studying the detailed shape of a RT distribution (Holden et al., 2009).
- 179 2. RT distributions may differ from each other in multiple ways, and hazard functions
180 allow one to capture these differences which mean-average comparisons may conceal
181 (Townsend, 1990).
- 182 3. EHA takes account of more of the data collected in a typical speeded response
183 experiment, by virtue of not discarding right-censored observations. Trials with very
184 long RTs are not discarded, but instead contribute to the risk set in each time bin
185 (see section 4.1.2 below).
- 186 4. Hazard modeling allows one to incorporate time-varying explanatory covariates, such
187 as heart rate, electroencephalogram (EEG) signal amplitude, gaze location, etc.
188 (Allison, 2010). This is useful for linking physiological effects to behavioral effects
189 when performing cognitive psychophysiology (Meyer, Osman, Irwin, & Yantis, 1988).
- 190 5. EHA can help to solve the problem of model mimicry, i.e., the fact that different
191 computational models can often predict the same mean RTs as observed in the
192 empirical data, but not necessarily the detailed shapes of the empirical RT hazard
193 distributions. As such, EHA can be a tool to help distinguish between competing
194 theories of cognition and brain function.

195 2.3 Event history analysis in the context of experimental psychology

196 To make EHA more relevant to researchers studying cognitive psychology and

197 cognitive neuroscience, in this section we provide a relevant worked example and consider
198 implications that are relevant to that domain of research.

199 **2.3.1 A worked example.** In the context of experimental psychology, it is

200 common for participants to be presented with either a 1-button detection task or a

201 discrimination task. For example, a task may involve choosing between two response
202 options with only one of them being correct. For such two-choice RT data, the
203 discrete-time EHA of the RT data (hazard and survivor functions) can be extended with a
204 discrete-time SAT analysis of the timed accuracy data. Specifically, the hazard function of
205 event occurrence can be extended with the discrete-time conditional accuracy function,
206 which gives you the probability that a response is correct given that it is emitted in time
207 bin t (Allison, 2010; Kantowitz & Pachella, 2021; Wickelgren, 1977). We refer to this
208 extended (hazard + conditional accuracy) analysis for choice RT data as EHA/SAT.

209 Integrating results between hazard and conditional accuracy functions for choice RT
210 data can be informative for understanding psychological processes. To illustrate, we
211 consider a hypothetical choice RT example that is inspired by real data (Panis & Schmidt,
212 2016), but simplified to make the main point clearer (Figure 3). In a standard priming
213 paradigm, there is a prime stimulus (e.g., an arrow pointing left or right) followed by a
214 target stimulus (another arrow pointing left or right). The prime can then be congruent or
215 incongruent with the target.

216 Figure 3 shows that the early upswing in hazard is equal for both priming conditions
217 (Figure 3, upper panel), and that early emitted responses are always correct in the
218 congruent condition and always incorrect in the incongruent condition (Figure 3, lower
219 panel). These results show that for short waiting times (< bin 6), responses always follow
220 the prime (and not the target, as instructed). During timebin 6 the target-triggered
221 response channel is activated and causes response competition – $ca(6) = .5$ – and a lower
222 hazard probability in the incongruent condition. For waiting times of 600 ms or more, the
223 hazard of response occurrence is lower in incongruent compared to congruent trials, and all
224 responses emitted in these late bins are correct.

225 This joint pattern of results is interesting because it can provide meaningfully
226 different conclusions about psychological processes compared to conventional analyses, such

as computing mean-average RT and accuracy across trials. Mean-average RT would only represent the overall ability of cognition to overcome interference, on average, across trials. For instance, if mean-average RT was higher in incongruent than congruent trials, one may conclude that cognitive mechanisms that support interference control are working as expected across trials, and are indexed by each recorded response. But such a conclusion is not supported when the effects are explored over a timeline. Instead, the psychological conclusion is much more nuanced and suggests that multiple states start, stop and possibly interact over a particular temporal window.

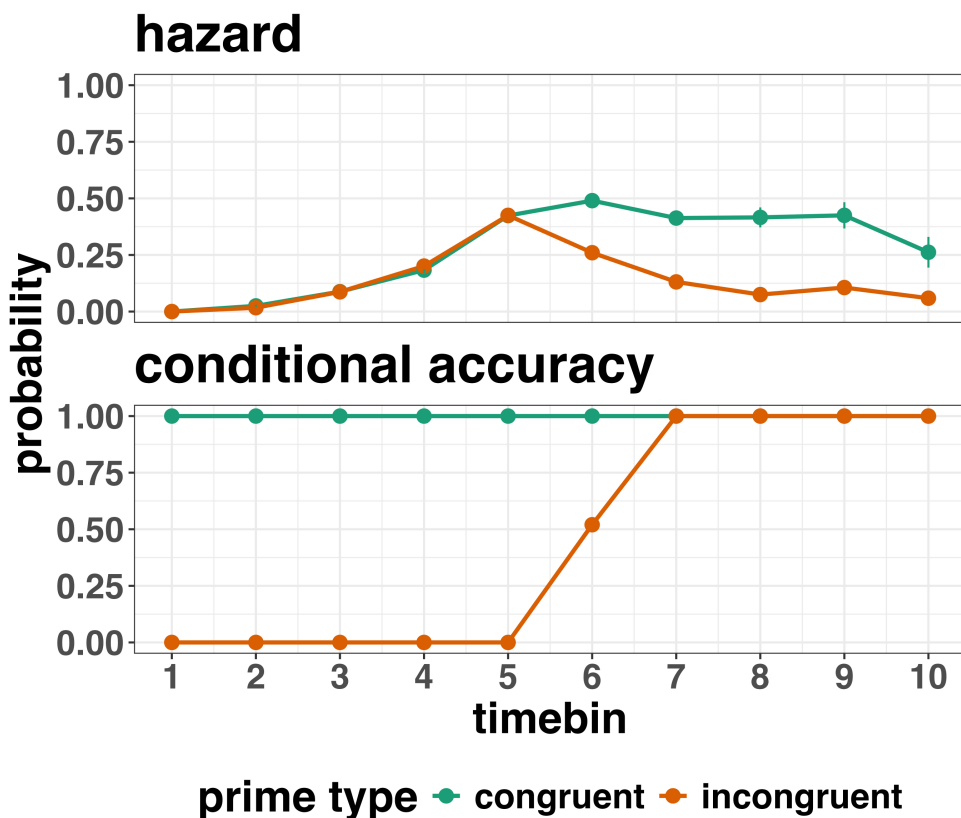


Figure 3. Discrete-time hazard and conditional accuracy functions. Discrete time-to-event and conditional accuracy data were simulated for 2000 trials for each of two priming conditions (congruent and incongruent prime stimuli). Error bars represent ± 1 standard error of the respective proportion. Bin width equals 100 ms.

Unlocking the temporal states of cognitive processes can be revealing for theory development and the understanding of basic psychological processes. Possibly more importantly, however, is that it simultaneously opens the door to address many new and previously unanswered questions. Do all participants show similar temporal states or are there individual differences? Do such individual differences extend to those individuals that have been diagnosed with some form of psychopathology? How do temporal states relate to brain-based mechanisms that might be studied using other methods from cognitive neuroscience? And how much of theory in cognitive psychology would be in need of revision if mean-average comparisons were supplemented with a temporal states approach?

2.3.2 Implications for designing experiments. Performing EHA in experimental psychology has implications for how experiments are designed. Indeed, if trials are categorised as a function of when responses occur, then each timebin will only include a subset of the total number of trials. For example, let's consider an experiment where each participant performs 2 conditions and there are 100 trial repetitions per condition. Those 100 trials must be distributed in some manner across the chosen number of bins.

In such experimental designs, since the number of trials per condition are spread across bins, it is important to have a relatively large number of trial repetitions per participant and per condition. Accordingly, experimental designs using this approach typically focus on factorial, within-subject designs, in which a large number of observations are made on a relatively small number of participants (so-called small- N designs). This approach emphasizes the precision and reproducibility of data patterns at the individual participant level to increase the inferential validity of the design (Baker et al., 2021; Smith & Little, 2018).

In contrast to the large- N design that typically average across many participants without being able to scrutinize individual data patterns, small- N designs retain crucial information about the data patterns of individual observers. This can be advantageous

262 whenever participants differ systematically in their strategies or in the time courses of their
263 effects, so that averaging them would lead to misleading data patterns. Note that because
264 statistical power derives both from the number of participants and from the number of
265 repeated measures per participant and condition, small- N designs can still achieve what
266 are generally considered acceptable levels of statistical power, if they have a sufficient
267 amount of data overall (Baker et al., 2021; Smith & Little, 2018).

268 **3. An overview of the general analytical workflow**

269 Although the focus is on EHA/SAT, we also want to briefly comment on broader
270 aspects of our general analytical workflow, which relate more to data science and data
271 analysis workflows.

272 **3.1 Data science workflow and descriptive statistics**

273 We perform data wrangling following tidyverse principles and a functional
274 programming approach (Wickham, Çetinkaya-Rundel, & Grolemund, 2023). In short,
275 functional programming means that you avoid writing your own loops and instead use
276 functions that have been built and tested by others. In addition, we also supply a set of
277 custom-built functions, which make the process of data wrangling in the context of data
278 preparation and descriptive statistics a lot quicker and more efficient.

279 **3.2 Inferential statistical approach**

280 Our lab adopts an estimation approach to multilevel regression (Kruschke & Liddell,
281 2018; Winter, 2019), which is heavily influenced by the Bayesian framework as suggested
282 by Richard McElreath (Kurz, 2023b; McElreath, 2020). We also use a “keep it maximal”
283 approach to specifying varying (or random) effects (Barr, Levy, Scheepers, & Tily, 2013).
284 This means that wherever possible we include varying intercepts and slopes per participant.

285 To make inferences, we use two main approaches. We compare models of different
 286 complexity, using information criteria (e.g., WAIC) and cross-validation (e.g., LOO), to
 287 evaluate out-of-sample predictive accuracy (McElreath, 2020). We also take the most
 288 complex model and evaluate key parameters of interest using point and interval estimates.

289 **3.3 Implementation**

290 We used R (Version 4.4.0; R Core Team, 2024)¹ for all reported analyses. The
 291 content of the tutorials, in terms of EHA and multilevel regression modelling, is mainly
 292 based on Allison (2010), Singer and Willett (2003), McElreath (2020), Heiss (2021), Kurz
 293 (2023a), and Kurz (2023b).

294 **4. Tutorials**

295 Tutorials 1a and 1b show how to calculate and plot the descriptive statistics of
 296 EHA/SAT when there are one or two independent variables, respectively. Tutorials 2a and
 297 2b illustrate how to use Bayesian multilevel modeling to fit hazard and conditional

¹ We, furthermore, used the R-packages *bayesplot* (Version 1.11.1; Gabry, Simpson, Vehtari, Betancourt, & Gelman, 2019), *brms* (Version 2.21.0; Bürkner, 2017, 2018, 2021), *citr* (Version 0.3.2; Aust, 2019), *cmdstanr* (Version 0.8.1.9000; Gabry, Češnovar, Johnson, & Brønner, 2024), *dplyr* (Version 1.1.4; Wickham, François, Henry, Müller, & Vaughan, 2023), *forcats* (Version 1.0.0; Wickham, 2023a), *ggplot2* (Version 3.5.1; Wickham, 2016), *lme4* (Version 1.1.35.5; Bates, Mächler, Bolker, & Walker, 2015), *lubridate* (Version 1.9.3; Grolemund & Wickham, 2011), *Matrix* (Version 1.7.0; Bates, Maechler, & Jagan, 2024), *nlme* (Version 3.1.166; Pinheiro & Bates, 2000), *papaja* (Version 0.1.2.9000; Aust & Barth, 2023), *patchwork* (Version 1.2.0; Pedersen, 2024), *purrr* (Version 1.0.2; Wickham & Henry, 2023), *RColorBrewer* (Version 1.1.3; Neuwirth, 2022), *Rcpp* (Eddelbuettel & Balamuta, 2018; Version 1.0.12; Eddelbuettel & François, 2011), *readr* (Version 2.1.5; Wickham, Hester, & Bryan, 2024), *RJ-2021-048* (Bengtsson, 2021), *standist* (Version 0.0.0.9000; Girard, 2024), *stringr* (Version 1.5.1; Wickham, 2023b), *tibble* (Version 3.2.1; Müller & Wickham, 2023), *tidybayes* (Version 3.0.6; Kay, 2023), *tidyverse* (Version 2.0.0; Wickham et al., 2019), and *tinylabels* (Version 0.2.4; Barth, 2023).

accuracy models, respectively. Tutorials 3a and 3b show how to implement, respectively, multilevel models for hazard and conditional accuracy in the frequentist framework. Additionally, to further simplify the process for other users, the first two tutorials rely on a set of our own custom functions that make sub-processes easier to automate, such as data wrangling and plotting functions (see section B in the supplemental material for a list of the custom functions).

Our list of tutorials is as follows:

- 1a. Wrangle raw data and calculate descriptive stats for one independent variable
- 1b. Wrangle raw data and calculate descriptive stats for two independent variables
- 2a. Bayesian multilevel modeling for $h(t)$
- 2b. Bayesian multilevel modeling for $ca(t)$
- 3a. Frequentist multilevel modeling for $h(t)$
- 3b. Frequentist multilevel modeling for $ca(t)$
- 4. Simulation and power analysis for planning experiments

4.1 Tutorial 1a: Calculating descriptive statistics using a life table

4.1.1 Data wrangling aims.

Our data wrangling procedures serve two related purposes. First, we want to summarise and visualise descriptive statistics that relate to our main research questions about the time course of psychological processes, using a life table. A life table includes for each time bin, the risk set (i.e., the number of trials that are event-free at the start of the bin), the number of observed events, and the estimates of $h(t)$, $S(t)$, $P(t)$, possibly $ca(t)$, and their estimated standard errors (se).

Second, we want to produce two different data sets that can each be submitted to different types of inferential modelling approaches. The two types of data structure we label as ‘person-trial’ data and ‘person-trial-bin’ data. The ‘person-trial’ data (Table 1) will be familiar to most researchers who record behavioural responses from participants, as

³²³ it represents the measured RT and accuracy per trial within an experiment. This data set
³²⁴ is used when fitting conditional accuracy models (Tutorials 2b and 3b).

Table 1

Data structure for ‘person-trial’ data

pid	trial	condition	rt	accuracy
1	1	congruent	373.49	1
1	2	incongruent	431.31	1
1	3	congruent	455.43	0
1	4	incongruent	622.41	1
1	5	incongruent	535.98	1
1	6	incongruent	540.08	1
1	7	congruent	511.07	1
1	8	incongruent	444.42	1
1	9	congruent	678.69	1
1	10	congruent	549.79	1

Note. The first 10 trials for participant 1 are shown. These data are simulated and for illustrative purposes only.

³²⁵ In contrast, the ‘person-trial-bin’ data (Table 2) has a different, more extended
³²⁶ structure, which indicates in which bin a response occurred, if at all, in each trial.
³²⁷ Therefore, the ‘person-trial-bin’ data generates a 0 in each bin until an event occurs and
³²⁸ then it generates a 1 to signal an event has occurred in that bin. This data set is used
³²⁹ when fitting hazard models (Tutorials 2a and 3a). It is worth pointing out that there is no
³³⁰ requirement for an event to occur at all (in any bin), as maybe there was no response on
³³¹ that trial or the event occurred after the time window of interest. Likewise, when the event

³³² occurs in bin 1 there would only be one row of data for that trial in the person-trial-bin
³³³ data set.

Table 2

Data structure for ‘person-trial-bin’ data

pid	trial	condition	timebin	event
1	1	congruent	1	0
1	1	congruent	2	0
1	1	congruent	3	0
1	1	congruent	4	1
1	2	incongruent	1	0
1	2	incongruent	2	0
1	2	incongruent	3	0
1	2	incongruent	4	0
1	2	incongruent	5	1

Note. The first 2 trials for participant 1 from Table 1 are shown. The width of the time bins is 100 ms. These data are simulated and for illustrative purposes only.

³³⁴ **4.1.2 A real data wrangling example.** To illustrate how to quickly set up life
³³⁵ tables for calculating the descriptive statistics (functions of discrete time), we use a
³³⁶ published data set on masked response priming from Panis and Schmidt (2016). In their
³³⁷ first experiment, Panis and Schmidt (2016) presented a double arrow for 94 ms that
³³⁸ pointed left or right as the target stimulus with an onset at time point zero in each trial.
³³⁹ Participants had to indicate the direction in which the double arrow pointed using their
³⁴⁰ corresponding index finger, within 800 ms after target onset. Response time and accuracy

341 were recorded on each trial. Prime type (blank, congruent, incongruent) and mask type
 342 were manipulated. Here we focus on the subset of trials in which no mask was presented.
 343 The 13-ms prime stimulus was a double arrow presented 187 ms before target onset in the
 344 congruent (same direction as target) and incongruent (opposite direction as target) prime
 345 conditions.

346 There are several data wrangling steps to be taken. First, we need to load the data
 347 before we (a) supply required column names, and (b) specify the factor condition with the
 348 correct levels and labels.

349 The required column names are as follows:

- 350 • “pid”, indicating unique participant IDs;
- 351 • “trial”, indicating each unique trial per participant;
- 352 • “condition”, a factor indicating the levels of the independent variable (1, 2, ...) and
 the corresponding labels;
- 354 • “rt”, indicating the response times in ms;
- 355 • “acc”, indicating the accuracies (1/0).

356 In the code of Tutorial 1a, this is accomplished as follows.

```
data_wr<-read_csv("../Tutorial_1_descriptive_stats/data/DataExp1_6subjects_wrangled.csv")
colnames(data_wr) <- c("pid", "bl", "tr", "condition", "resp", "acc", "rt", "trial")
data_wr <- data_wr %>%
  mutate(condition = condition + 1, # original levels were 0, 1, 2.
        condition = factor(condition,
                            levels=c(1,2,3),
                            labels=c("blank", "congruent", "incongruent")))
```

357 Next, we can set up the life tables and plots of the discrete-time functions $h(t)$, $S(t)$,
 358 $ca(t)$, and $P(t)$ – see section A of the supplementary material for their definitions. To do so

359 using a functional programming approach, one has to nest the data within participants
 360 using the group_nest() function, and supply a user-defined censoring time and bin width
 361 to our custom function “censor()”, as follows.

```
data_nested <- data_wr %>% group_nest(pid)

data_final <- data_nested %>%
  # ! user input: censoring time, and bin width
  mutate(censored = map(data, censor, 600, 40)) %>%
  # create person-trial-bin data set
  mutate(ptb_data = map(censored, ptb)) %>%
  # create life tables without ca(t)
  mutate(lifetable = map(ptb_data, setup_lt)) %>%
  # calculate ca(t)
  mutate(condacc = map(censored, calc_ca)) %>%
  # create life tables with ca(t)
  mutate(lifetable_ca = map2(lifetable, condacc, join_lt_ca)) %>%
  # create plots
  mutate(plot = map2(.x = lifetable_ca, .y = pid, plot_eha,1))
```

362 Note that the censoring time should be a multiple of the bin width (both in ms). The
 363 censoring time should be a time point after which no informative responses are expected
 364 anymore. In experiments that implement a response deadline in each trial the censoring
 365 time can equal that deadline time point. Trials with a RT larger than the censoring time,
 366 or trials in which no response is emitted during the data collection period, are treated as
 367 right-censored observations in EHA. In other words, these trials are not discarded, because
 368 they contain the information that the event did not occur before the censoring time.
 369 Removing such trials before calculating the mean event time will result in underestimation
 370 of the true mean.

371 The person-trial-bin oriented data set is created by our custom function ptb(), and it
 372 has one row for each time bin (of each trial) that is at risk for event occurrence. The

373 variable “event” in the person-trial-bin oriented data set indicates whether a response
374 occurs (1) or not (0) for each bin.

375 The next step is to set up the life table using our custom function `setup_lt()`,
376 calculate the conditional accuracies using our custom function `calc_ca()`, add the `ca(t)`
377 estimates to the life table using our custom function `join_lt_ca()`, and then plot the
378 descriptive statistics using our custom function `plot_eha()`. When creating the plots, some
379 warning messages will likely be generated, like these:

- 380 • Removed 2 rows containing missing values or values outside the scale range
381 (`geom_line()`).
382 • Removed 2 rows containing missing values or values outside the scale range
383 (`geom_point()`).
384 • Removed 2 rows containing missing values or values outside the scale range
385 (`geom_segment()`).

386 The warning messages are generated because some bins have no hazard and `ca(t)`
387 estimates, and no error bars. They can thus safely be ignored. One can now inspect
388 different aspects, including the life table for a particular condition of a particular subject,
389 and a plot of the different functions for a particular participant. In general, it is important
390 to visually inspect the functions first for each participant, in order to identify individuals
391 that may be guessing (e.g., a flat conditional accuracy function at .5 indicates that
392 someone is just guessing), outlying individuals, and/or different groups with qualitatively
393 different behavior.

394 Table 3 shows the life table for condition “blank” (no prime stimulus presented) for
395 participant 6.

Table 3

The life table for the blank prime condition of participant 6.

bin	risk_set	events	hazard	se_haz	survival	se_surv	ca	se_ca
0	220	NA	NA	NA	1.00	0.00	NA	NA
40	220	0	0.00	0.00	1.00	0.00	NA	NA
80	220	0	0.00	0.00	1.00	0.00	NA	NA
120	220	0	0.00	0.00	1.00	0.00	NA	NA
160	220	0	0.00	0.00	1.00	0.00	NA	NA
200	220	0	0.00	0.00	1.00	0.00	NA	NA
240	220	0	0.00	0.00	1.00	0.00	NA	NA
280	220	7	0.03	0.01	0.97	0.01	0.29	0.17
320	213	13	0.06	0.02	0.91	0.02	0.77	0.12
360	200	26	0.13	0.02	0.79	0.03	0.92	0.05
400	174	40	0.23	0.03	0.61	0.03	1.00	0.00
440	134	48	0.36	0.04	0.39	0.03	0.98	0.02
480	86	37	0.43	0.05	0.22	0.03	1.00	0.00
520	49	32	0.65	0.07	0.08	0.02	1.00	0.00
560	17	9	0.53	0.12	0.04	0.01	1.00	0.00
600	8	4	0.50	0.18	0.02	0.01	1.00	0.00

Note. The column named “bin” indicates the endpoint of each time bin (in ms), and includes time point zero. For example the first bin is (0,40] with the starting point excluded and the endpoint included. At time point zero, no events can occur and therefore $h(t=0)$ and $ca(t=0)$ are undefined. $se =$ standard error. $ca =$ conditional accuracy. $NA =$ undefined.

Figure 4 displays the discrete-time hazard, survivor, conditional accuracy, and

397 probability mass functions for each prime condition for participant 6. By using
 398 discrete-time hazard functions of event occurrence – in combination with conditional
 399 accuracy functions for two-choice tasks – one can provide an unbiased, time-varying, and
 400 probabilistic description of the latency and accuracy of responses based on all trials of any
 401 data set.

Descriptive stats for subject 6

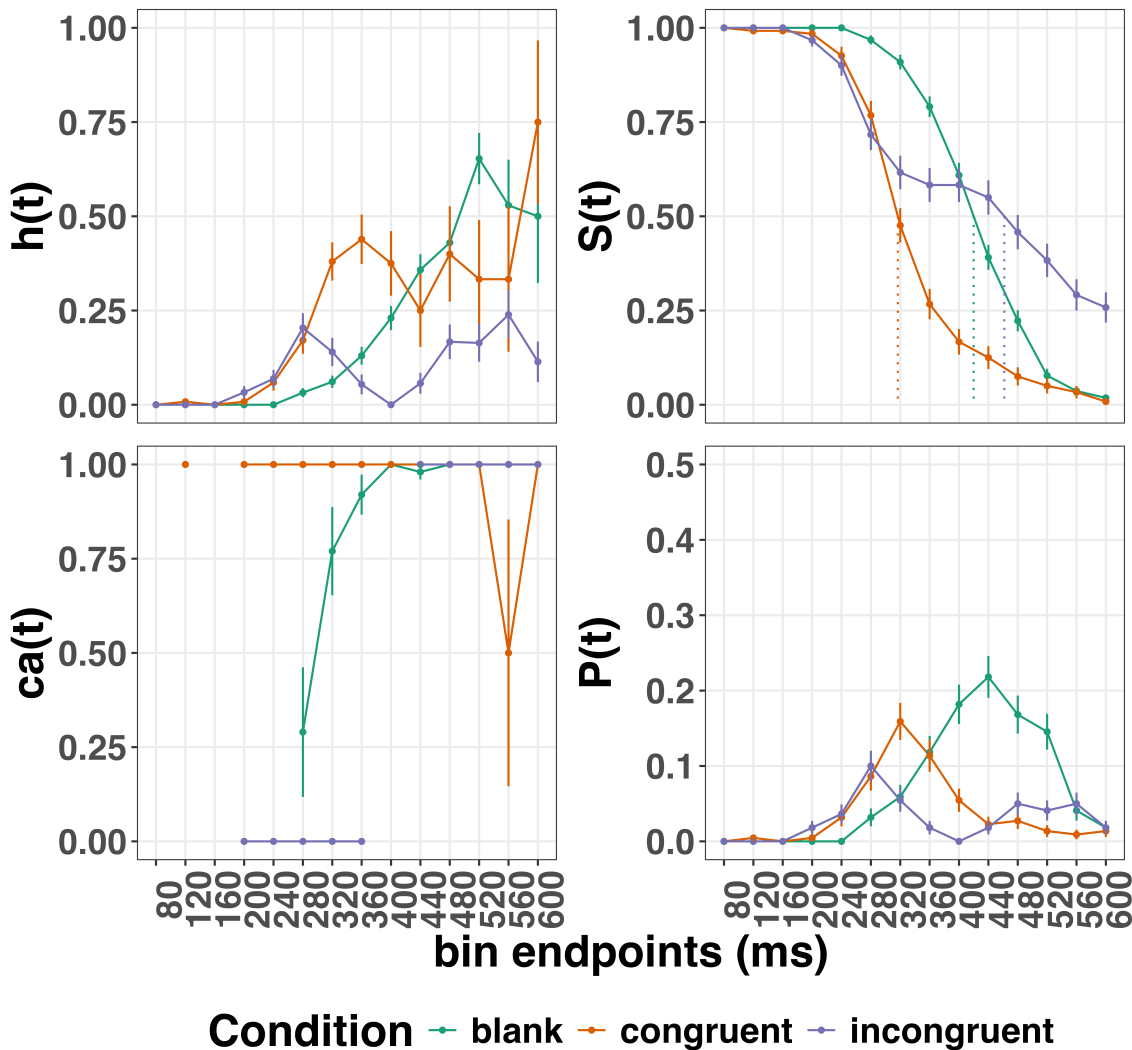


Figure 4. Estimated discrete-time hazard (h), survivor (S), conditional accuracy (ca) and probability mass (P) functions for participant 6. Vertical dotted lines indicate the estimated median RTs. Error bars represent ± 1 standard error of the respective proportion.

402 For example, for participant 6, the estimated hazard values in bin (240,280] are 0.03,

403 0.17, and 0.20 for the blank, congruent, and incongruent prime conditions, respectively. In

404 other words, when the waiting time has increased until *240 ms* after target onset, then the

405 conditional probability of response occurrence in the next 40 ms is more than five times

406 larger for both prime-present conditions, compared to the blank prime condition.

407 Furthermore, the estimated conditional accuracy values in bin (240,280] are 0.29, 1,

408 and 0 for the blank, congruent, and incongruent prime conditions, respectively. In other

409 words, if a response is emitted in bin (240,280], then the probability that it is correct is

410 estimated to be 0.29, 1, and 0 for the blank, congruent, and incongruent prime conditions,

411 respectively.

412 However, when the waiting time has increased until *400 ms* after target onset, then

413 the conditional probability of response occurrence in the next 40 ms is estimated to be

414 0.36, 0.25, and 0.06 for the blank, congruent, and incongruent prime conditions,

415 respectively. And when a response does occur in bin (400,440], then the probability that it

416 is correct is estimated to be 0.98, 1, and 1 for the blank, congruent, and incongruent prime

417 conditions, respectively.

418 These distributional results suggest that participant 6 is initially responding to the

419 prime even though (s)he was instructed to only respond to the target, that response

420 competition emerges in the incongruent prime condition around 300 ms, and that only

421 slower responses are fully controlled by the target stimulus. Qualitatively similar results

422 were obtained for the other five participants. When participants show qualitatively similar

423 distributional patterns, one might consider aggregating their data and plotting the

424 group-average distribution per condition (see Tutorial_1a.Rmd).

425 In general, these results go against the (often implicit) assumption in research on

426 priming that all observed responses are primed responses to the target stimulus. Instead,

427 the distributional data show that early responses are triggered exclusively by the prime

428 stimulus, while only later responses reflect primed responses to the target stimulus.

429 At this point, we have calculated, summarised and plotted descriptive statistics for
430 the key variables in EHA/SAT. As we will show in later Tutorials, statistical models for
431 $h(t)$ and $ca(t)$ can be implemented as generalized linear mixed regression models predicting
432 event occurrence (1/0) and conditional accuracy (1/0) in each bin of a selected time
433 window for analysis. But first we consider calculating the descriptive statistics for two
434 independent variables.

435 **4.2 Tutorial 1b: Generalising to a more complex design**

436 So far in this paper, we have used a simple experimental design, which involved one
437 condition with three levels. But psychological experiments are often more complex, with
438 crossed factorial designs and/or conditions with more than three levels. The purpose of
439 Tutorial 1b, therefore, is to provide a generalisation of the basic approach, which extends
440 to a more complicated design. We felt that this might be useful for researchers in
441 experimental psychology that typically use crossed factorial designs.

442 To this end, Tutorial 1b illustrates how to calculate and plot the descriptive statistics
443 for the full data set of Experiment 1 of Panis and Schmidt (2016), which includes two
444 independent variables: mask type and prime type. As we use the same functional
445 programming approach as in Tutorial 1a, we simply present the sample-based functions for
446 each participant as part of Tutorial_1b.Rmd for those that are interested.

447 **4.3 Tutorial 2a: Fitting Bayesian hazard models to discrete time-to-event data**

448 In this third tutorial, we illustrate how to fit Bayesian multilevel regression models to
449 the RT data of the masked response priming data used in Tutorial 1a. Fitting (Bayesian or
450 non-Bayesian) regression models to time-to-event data is important when you want to
451 study how the shape of the hazard function depends on various predictors (Singer &

452 Willett, 2003).

453 **4.3.1 Hazard model considerations.** There are several analytic decisions one
454 has to make when fitting a discrete-time hazard model. First, one has to select an analysis
455 time window, i.e., a contiguous set of bins for which there is enough data for each
456 participant. Second, given that the dependent variable (event occurrence) is binary, one
457 has to select a link function (see section C in the supplementary material). The cloglog link
458 is preferred over the logit link when events can occur in principle at any time point within
459 a bin, which is the case for RT data (Singer & Willett, 2003). Third, one has to choose
460 whether to treat TIME (i.e., the time bin index t) as a categorical or continuous predictor.
461 And when you treat a variable as a categorical predictor, you can choose between reference
462 coding and index coding. With reference coding, one defines the variable as a factor and
463 selects one of the k categories as the reference level. Brm() will then construct $k-1$
464 indicator variables (see model M1d in Tutorial_2a.Rmd for an example). With index
465 coding, one constructs an index variable that contains integers that correspond to different
466 categories (see models M0i and M1i below). As explained by McElreath (2020), the
467 advantage of index coding is that the same prior can be assigned to each level of the index
468 variable, so that each category has the same prior uncertainty.

469 In the case of a large- N design without repeated measurements, the parameters of a
470 discrete-time hazard model can be estimated using standard logistic regression software
471 after expanding the typical person-trial data set into a person-trial-bin data set (Allison,
472 2010). When there is clustering in the data, as in the case of a small- N design with
473 repeated measurements, the parameters of a discrete-time hazard model can be estimated
474 using population-averaged methods (e.g., Generalized Estimating Equations), and Bayesian
475 or frequentist generalized linear mixed models (Allison, 2010).

476 In general, there are three assumptions one can make or relax when adding
477 experimental predictor variables and other covariates: The linearity assumption for
478 continuous predictors (the effect of a 1 unit change is the same anywhere on the scale), the

479 additivity assumption (predictors do not interact), and the proportionality assumption
 480 (predictors do not interact with TIME).

481 In tutorial_2a.Rmd we fit several Bayesian multilevel models (i.e., generalized linear
 482 mixed models) that differ in complexity to the person-trial-bin oriented data set that we
 483 created in Tutorial 1a. We decided to select the analysis time window (200,600] and the
 484 cloglog link. Below, we shortly discuss two of these models. The person-trial-bin data set is
 485 prepared as follows.

```
# read in the file we saved in tutorial 1a
ptb_data <- read_csv("Tutorial_1_descriptive_stats/data/inputfile_hazard_modeling.csv")

ptb_data <- ptb_data %>%
  # select analysis time range: (200,600] with 10 bins (time bin ranks 6 to 15)
  filter(period > 5) %>%
    # define categorical predictor TIME as index variable named timebin
  mutate(timebin = factor(period, levels = c(6:15)),
    # factor "condition" using reference coding, with "blank" as the reference level
    condition = factor(condition, labels = c("blank", "congruent", "incongruent")),
    # categorical predictor "prime" with index coding
    prime = ifelse(condition=="blank", 1, ifelse(condition=="congruent", 2, 3)),
    prime = factor(prime, levels = c(1,2,3)))
```

486 **4.3.2 Prior distributions.** To get the posterior distribution of each model
 487 parameter given the data, we need to specify prior distributions for the model parameters
 488 which reflect our prior beliefs. In Tutorial_2a.Rmd we perform a few prior predictive
 489 checks to make sure our selected prior distributions reflect our prior beliefs (Gelman,
 490 Vehtari, et al., 2020).

491 The middle column of Figure 15 in section E of the supplementary material shows six
 492 examples of prior distributions for an intercept on the logit and/or cloglog scales. While a
 493 normal distribution with relatively large variance is often used as a weakly informative

494 prior for continuous dependent variables, rows A and B in Figure 15 show that specifying
 495 such distributions on the logit and cloglog scales actually leads to rather informative
 496 distributions on the original probability scale, as most mass is pushed to probabilities of 0
 497 and 1.

498 **4.3.3 Model M0i: A null model with index coding.** When you do not want to
 499 make assumptions about the shape of the hazard function, or its shape is not smooth but
 500 irregular, then you can use a general specification of TIME, i.e., fit one grand intercept per
 501 time bin. In this first model, we use a general specification of TIME using index coding,
 502 and do not include experimental predictors. We call this model “M0i”.

503 Before we fit model M0i, we select the necessary columns from the data, and specify
 504 our priors. In the code of Tutorial 2a, model M0i is specified as follows.

```
model_M0i <-
  brm(data = data_M0i,
       family = bernoulli(link="cloglog"),
       formula = event ~ 0 + timebin + (0 + timebin | pid),
       prior = priors_M0i,
       chains = 4, cores = 4,
       iter = 3000, warmup = 1000,
       control = list(adapt_delta = 0.999,
                      step_size = 0.04,
                      max_treedepth = 12),
       seed = 12, init = "0",
       file = "Tutorial_2_Bayesian/models/model_M0i")
```

505 After selecting the bernoulli family and the cloglog link, the model formula is
 506 specified. The specification “ $0 + \dots$ ” removes the default intercept in brm(). The fixed
 507 effects include an intercept for each level of timebin. Each of these intercepts is allowed to

508 vary across individuals (variable pid). We request 2000 samples from the posterior
 509 distribution for each of four chains. Estimating model M0i took about 30 minutes on a
 510 MacBook Pro (Sonoma 14.6.1 OS, 18GB Memory, M3 Pro Chip).

511 **4.3.4 Model M1i: Adding the effects of prime-target congruency.** Previous
 512 research has shown that psychological effects typically change over time (Panis, 2020;
 513 Panis, Moran, et al., 2020; Panis & Schmidt, 2022; Panis et al., 2017; Panis & Wagemans,
 514 2009). In the next model, therefore, we use index coding for both TIME (variable
 515 “timebin”) and the categorical predictor prime-target-congruency (variable “prime”), so
 516 that we get 30 grand intercepts, one for each combination of timebin level and prime level.
 517 Here is the model formula of this model that we call “M1i”.

```
event ~ 0 + timebin:prime + (0 + timebin:prime | pid)
```

518 Estimating model M1i took about 124 minutes.

519 **4.3.5 Compare the models.** We can compare the two models using the Widely
 520 Applicable Information Criterion (WAIC) and Leave-One-Out (LOO) cross-validation, and
 521 look at model weights for both criteria (Kurz, 2023a; McElreath, 2020).

```
model_weights(model_M0i, model_M1i, weights = "loo") %>% round(digits = 2)
```

```
522 ## model_M0i model_M1i
523 ## 0 1
```

```
model_weights(model_M0i, model_M1i, weights = "waic") %>% round(digits = 2)
```

```
524 ## model_M0i model_M1i
525 ## 0 1
```

526 Clearly, both the loo and waic weighting schemes assign a weight of 1 to model M1i,
 527 and a weight of 0 to the other simpler model.

528 **4.3.6 Evaluating parameter estimates in model M1i.** To make inferences

529 from the parameter estimates in model M1i, we first plot the densities of the draws from
 530 the posterior distributions of its population-level parameters in Figure 5, together with
 531 point (median) and interval estimates (80% and 95% credible intervals).

Posterior distributions for population-level effects in Model M1i

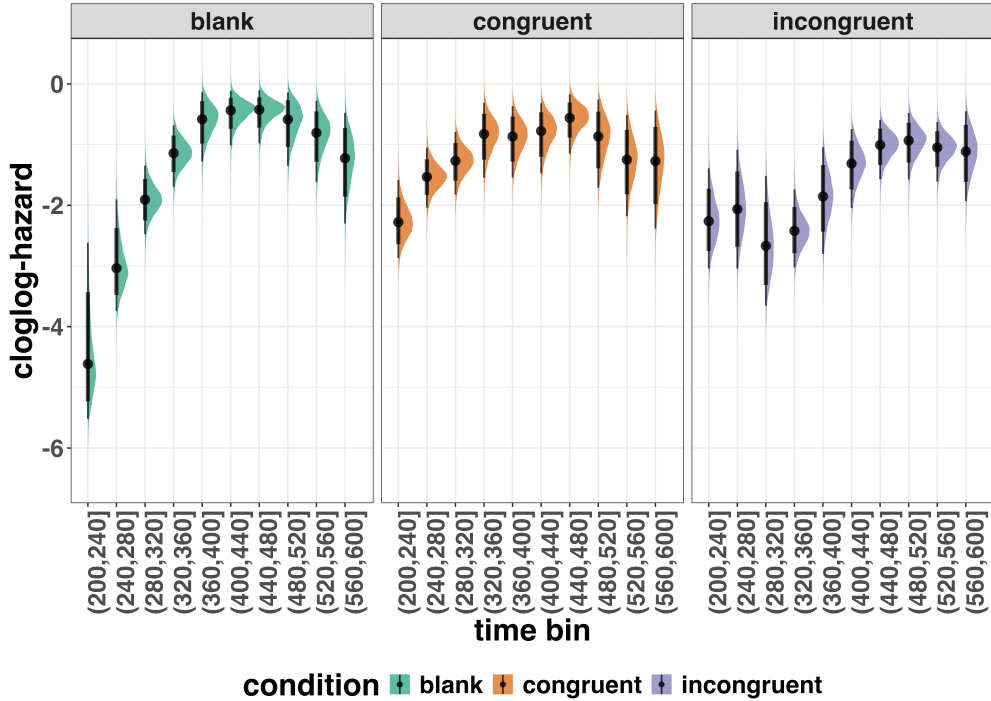


Figure 5. Medians and 80/95% credible intervals of the posterior distributions of the population-level parameters of model M1i.

532 Because the parameter estimates are on the cloglog-hazard scale, we can ease our

533 interpretation by plotting the expected value of the posterior predictive distribution – the
 534 predicted hazard values – for the grand average (Figure 6A), and for each participant in
 535 the data set (Figure 6B).

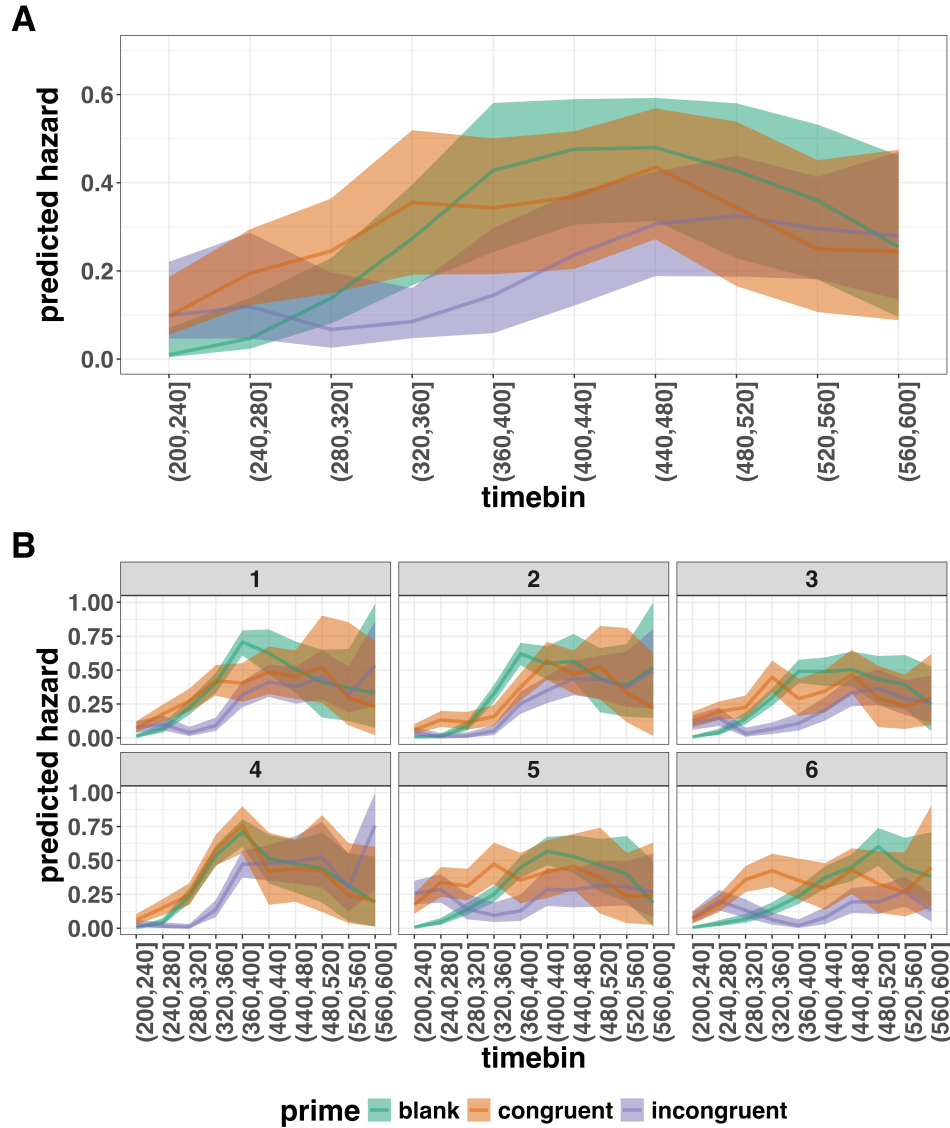


Figure 6. Point (median) and 80/95% credible interval summaries of the hazard estimates (expected values of the draws from the posterior predictive distributions) in each time bin for the grand average (A), and for each participant (B).

536 As we are actually interested in the effects of congruent and incongruent primes,

537 relative to the blank prime condition, we can construct two contrasts (congruent-blank,
 538 incongruent-blank), and plot the posterior distributions of these contrast effects, both for
 539 the grand average (Figure 7A; grand average marginal effect) and for each participant in

540 the data set (Figure 7B; subject-specific average marginal effect).

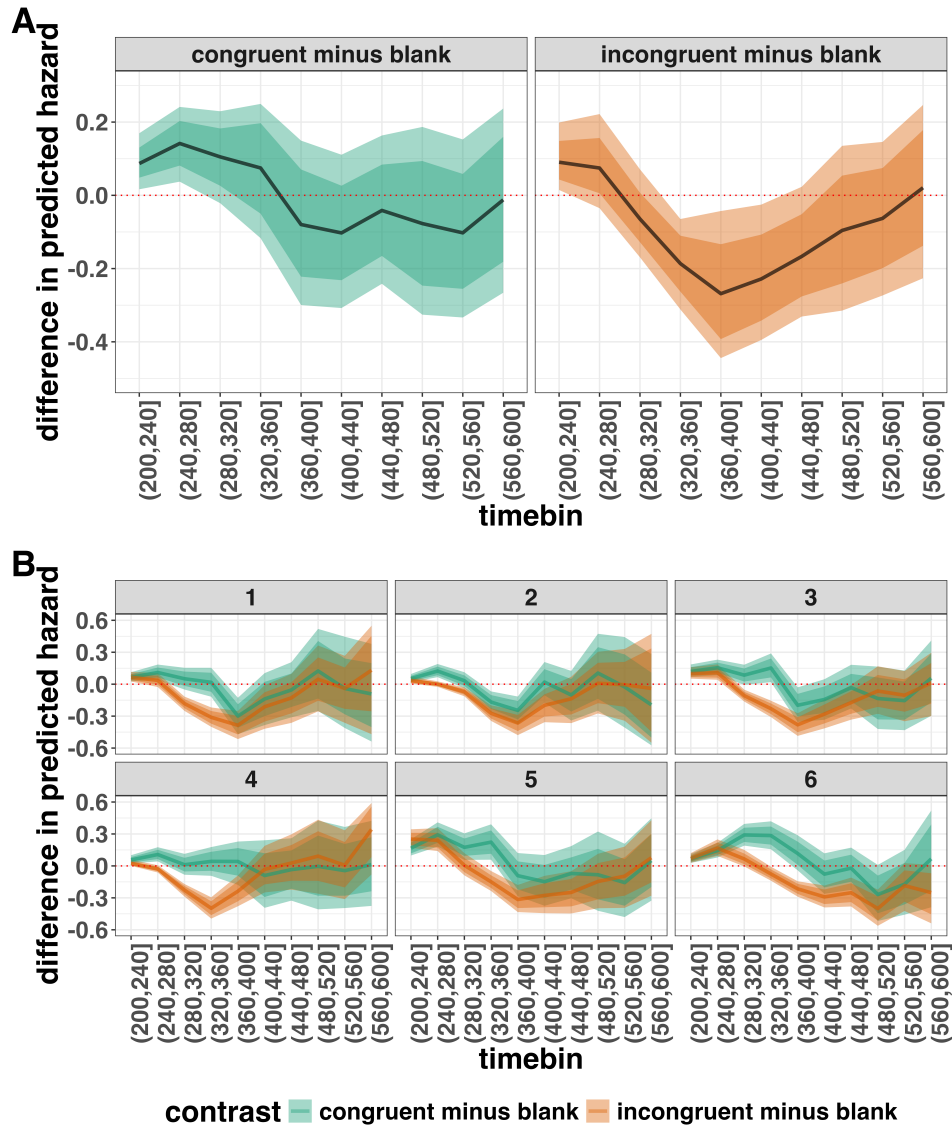


Figure 7. Point (mean) and 80/95% credible interval summaries of estimated differences in hazard in each time bin for the grand average (A), and for each participant (B).

541 The point estimates and quantile intervals can be reported in a table (see
 542 Tutorial_2a.Rmd for details).

543 **Example conclusions for M1i.** What can we conclude from model M1i about
 544 our research question, i.e., the temporal dynamics of the effect of prime-target congruency

545 on RT? In other words, in which of the 40-ms time bins between 200 and 600 ms after
546 target onset does changing the prime from blank to congruent or incongruent affect the
547 hazard of response occurrence (for a prime-target SOA of 187 ms)?

548 If we want to estimate the population-level effect of prime type on hazard, we can
549 base our conclusion on Figure 7A. The contrast “congruent minus blank” was estimated to
550 be 0.09 hazard units in bin (200,240] (95% CrI = [0.02, 0.17]), and 0.14 hazard units in bin
551 (240,280]) (95% CrI = [0.04, 0.25]). For the other bins, the 95% credible interval contained
552 zero. The contrast “incongruent minus blank” was estimated to be 0.09 hazard units in bin
553 (200,240] (95% CrI = [0.01, 0.21]), -0.19 hazard units in bin (320,360] (95% CrI = [-0.31,
554 -0.06]), -0.27 hazard units in bin (360,400] (95% CrI = [-0.45, -0.04]), and -0.23 hazard
555 units in bin (400,440] (95% CrI = [-0.40, -0.03]). For the other bins, the 95% credible
556 interval contained zero.

557 There are thus two phases of performance for the average person between 200 and
558 600 ms after target onset. In the first phase, the addition of a congruent or incongruent
559 prime stimulus increases the hazard of response occurrence compared to blank prime trials
560 in the time period (200, 240]. In the second phase, only the incongruent prime decreases
561 the hazard of response occurrence compared to blank primes, in the time period (320,440].
562 The sign of the effect of incongruent primes on the hazard of response occurrence thus
563 depends on how much waiting time has passed since target onset.

564 If we want to focus more on inter-individual differences, we can study the
565 subject-specific hazard functions in Figure 7B. Note that three participants (1, 2, and 3)
566 show a negative difference for the contrast “congruent minus incongruent” in bin (360,400]
567 – subject 2 also in bin (320,360].

568 Future studies could (a) increase the number of participants to estimate the
569 proportion of “dippers” in the subject population, and/or (b) try to explain why this dip
570 occurs. For example, Panis and Schmidt (2016) concluded that active, top-down,

571 task-guided response inhibition effects emerge around 360 ms after the onset of the stimulus
572 following the prime (here: the target stimulus). Such a top-down inhibitory effect might
573 exist in our priming data set, because after some time participants will learn that the first
574 stimulus is not the one they have to respond to. To prevent a premature overt response to
575 the prime they thus might gradually increase a global response threshold during the
576 remainder of the experiment, which could result in a lower hazard in congruent trials
577 compared to blank trials, for bins after ~360 ms, and towards the end of the experiment.
578 This effect might be masked for incongruent primes by the response competition effect.

579 Interestingly, all subjects show a tendency in their mean difference (congruent minus
580 blank) to “dip” around that time (Figure 7B). Therefore, future modeling efforts could
581 incorporate the trial number into the model formula, in order to also study how the effects
582 of prime type on hazard change on the long experiment-wide time scale, next to the short
583 trial-wide time scale. In Tutorial_2a.Rmd we provide a number of model formulae that
584 should get you going.

585 4.4 Tutorial 2b: Fitting Bayesian conditional accuracy models

586 In this fourth tutorial, we illustrate how to fit a Bayesian multilevel regression model
587 to the timed accuracy data from the masked response priming data used in Tutorial 1a.
588 The general process is similar to Tutorial 2a, except that (a) we use the person-trial data,
589 (b) we use the logit link function, and (c) we change the priors. To keep the tutorial short,
590 we only fit one conditional accuracy model, which was based on model M1i from Tutorial
591 2a and labelled M1i_ca.

592 To make inferences from the parameter estimates in model M1i_ca, we first plot the
593 densities of the draws from the posterior distributions of its population-level parameters in
594 Figure 8, together with point (median) and interval estimates (80% and 95% credible
595 intervals).

Posterior distributions for population-level effects in Model M1i_ca

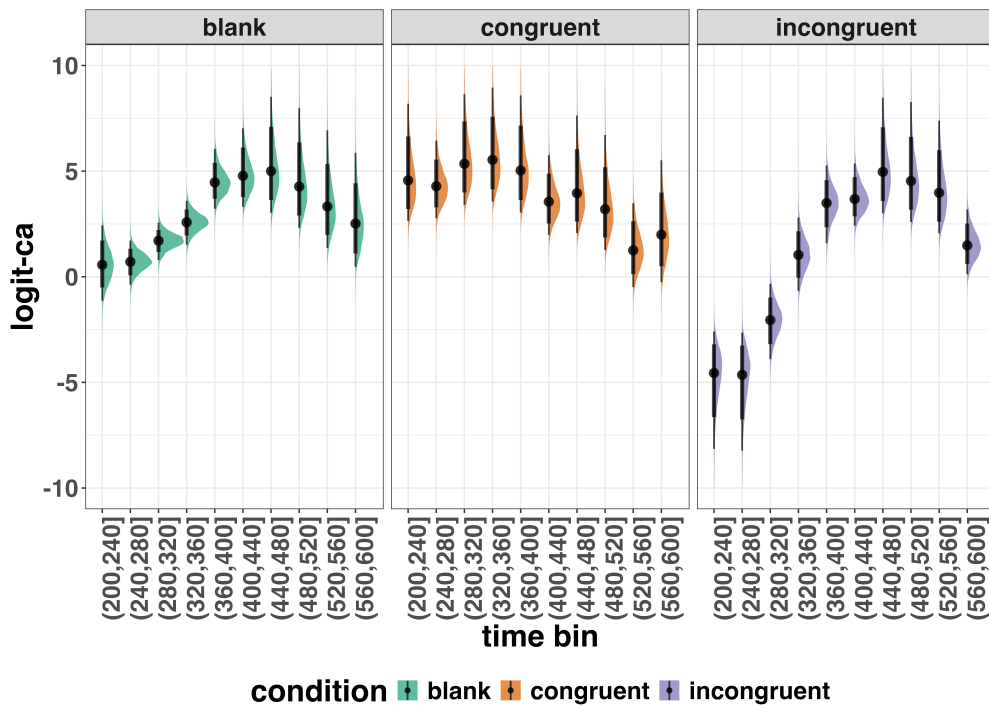


Figure 8. Medians and 80/95% credible intervals of the posterior distributions of the population-level parameters of model M1i_ca. ca = conditional accuracy.

Because the parameter estimates are on the logit-ca scale, we can ease our

interpretation by plotting the expected value of the posterior predictive distribution – the predicted conditional accuracies – for the grand average (Figure 9A), and for each participant in the data set (Figure 9B).

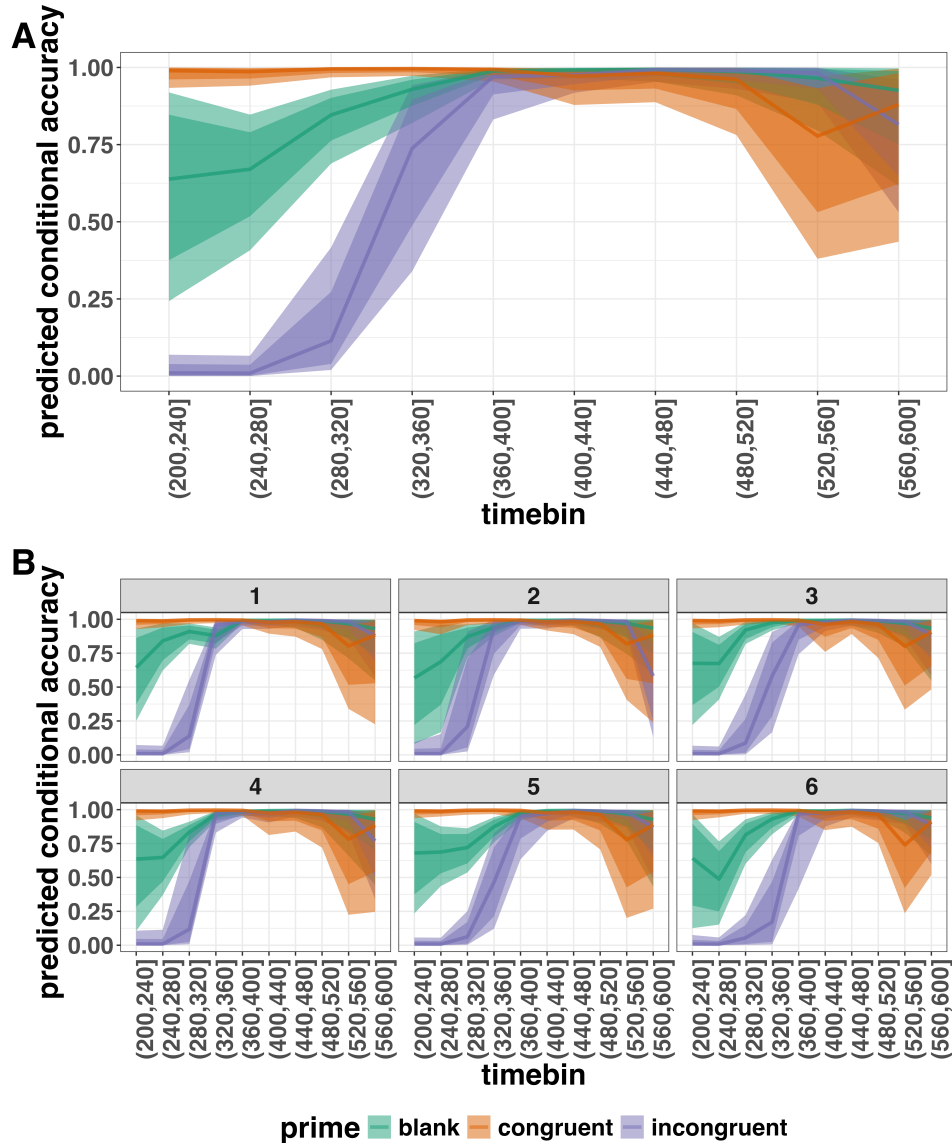


Figure 9. Point (median) and 80/95% credible interval summaries of the conditional accuracy estimates (expected values of the draws from the posterior predictive distributions) in each time bin for the grand average (A), and for each participant (B).

As we are actually interested in the effects of congruent and incongruent primes,

relative to the blank prime condition, we can construct two contrasts (congruent-blank, incongruent-blank), and plot the posterior distributions of these contrast effects for the grand average (Figure 10; grand average marginal effect).

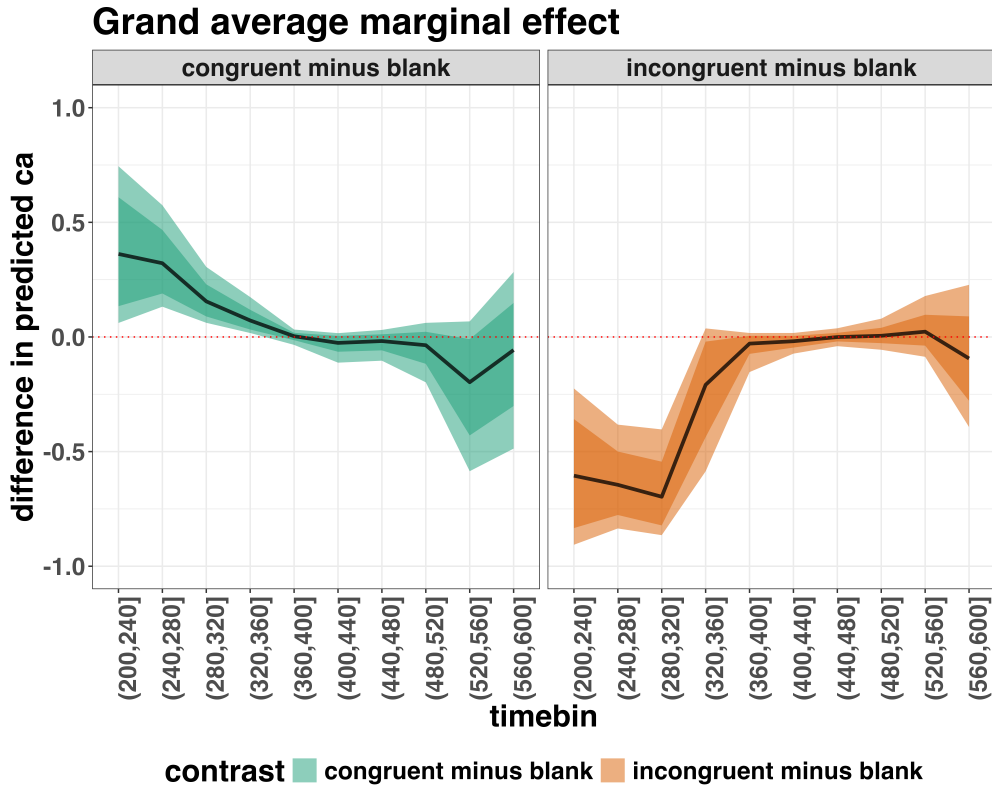


Figure 10. Point (mean) and 80/95% credible interval summaries of estimated differences in conditional accuracy in each time bin for the grand average.

604 Based on Figure 10 we see that congruent primes have a positive effect on the
 605 conditional accuracy of emitted responses in time bins (200,240], (240,280], and (280,320],
 606 relative to the estimates in the baseline condition (blank prime; red dashed lines in Figure
 607 10). Incongruent primes have a negative effect on the conditional accuracy of emitted
 608 responses in those time bins, relative to the estimates in the baseline condition.

609 **4.5 Tutorial 3a: Fitting Frequentist hazard models**

610 In this fifth tutorial we illustrate how to fit a multilevel regression model to RT data
 611 in the frequentist framework, for the data used in Tutorial 1a. The general process is
 612 similar to that in Tutorial 2a, except that there are no priors to set.

613 Again, to keep the tutorial concise, we only fit model M1i (see Tutorial 2a) using the

614 function `glmer()` from the R package `lme4`. Alternatively, one could also use the function
 615 `glmmPQL()` from the R package `MASS` (Ripley et al., 2024). The resulting hazard model
 616 is called `M1i_f` with the appended “`_f`” denoting a frequentist model.

617 In Figure 11 we compare the parameter estimates from the Bayesian regression model
 618 `M1i` with those from the frequentist model `M1i_f`.

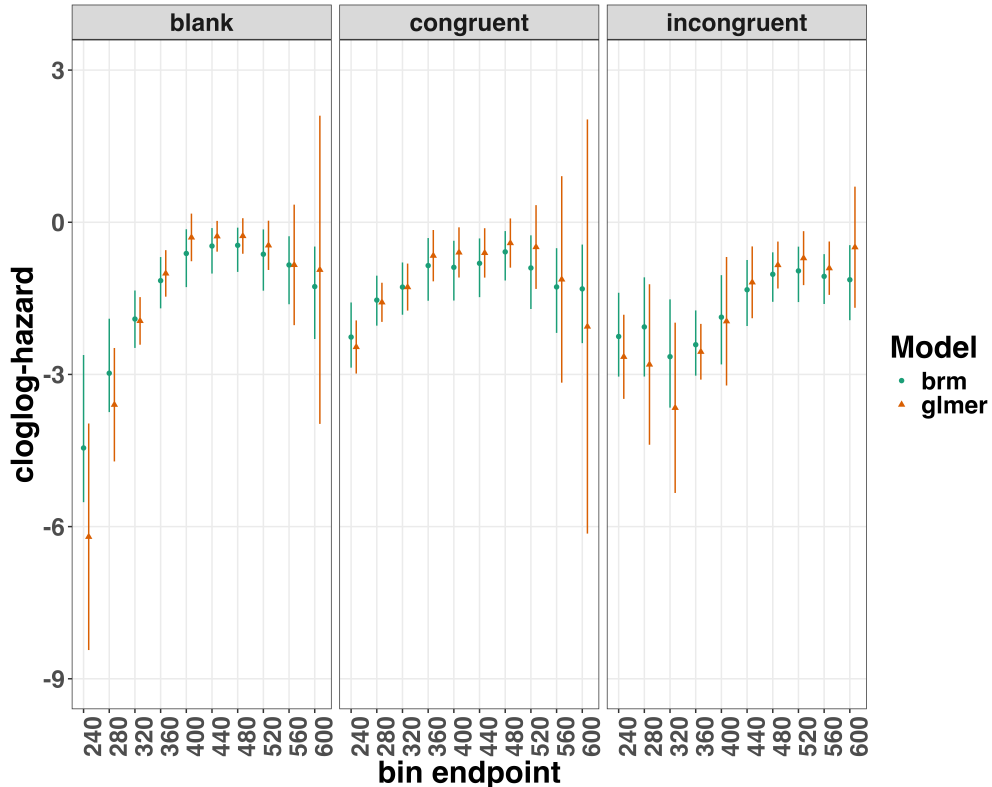


Figure 11. Parameter estimates for model `M1i` from `brm()` – means and 95% credible intervals – and model `M1i_f` from `glmer()` – maximum likelihood estimates and 95% confidence intervals.

619 Figure 11 confirms that the parameter estimates from both Bayesian and frequentist
 620 models are pretty similar, which makes sense given the close similarity in model structure.
 621 However, model `M1i_f` did not converge and resulted in a singular fit. This is of course one
 622 of the reasons why Bayesian modeling has become so popular in recent years. But the price
 623 you pay for being able to fit models with more complex varying effects structures via a

624 Bayesian framework is increased computation time. In other words, as we have noted
625 throughout, some of the Bayesian models in Tutorials 2a took several hours to build.

626 **4.6 Tutorial 3b: Fitting Frequentist conditional accuracy models**

627 In this sixth tutorial we illustrate how to fit a multilevel regression model to the
628 timed accuracy data in the frequentist framework, for the data used in Tutorial 1a. To be
629 concise, we only fit effects from model M1i_ca (see Tutorial 2b) using the function glmer()
630 from the R package lme4. Alternatively, one could also use the function glmmPQL() from
631 the R package MASS (Ripley et al., 2024). The resulting conditional accuracy model,
632 which we labelled M1i_ca_f, did not converge and resulted in a singular fit. Again, this
633 just highlights some of the difficulties in fitting reasonably complex varying/random effects
634 structures in frequentist workflows.

635 **4.7 Tutorial 4: Planning**

636 In the final tutorial, we look at planning a future experiment, which uses EHA.

637 **4.7.1 Background.** The general approach to planning that we adopt here involves
638 simulating reasonably structured data to help guide what you might be able to expect from
639 your data once you collect it (Gelman, Vehtari, et al., 2020). The basic structure and code
640 follows the examples outlined by Solomon Kurz in his ‘power’ blog posts
641 (<https://solomonkurz.netlify.app/blog/bayesian-power-analysis-part-i/>) and Lisa
642 Debruine’s R package faux{} (<https://debruine.github.io/faux/>) as well as the related
643 paper (DeBruine & Barr, 2021).

644 **4.7.2 Basic workflow.** The basic workflow is as follows:

- 645 1. Fit a regression model to existing data.
646 2. Use the regression model parameters to simulate new data.

- 647 3. Write a function to create 1000s of datasets and vary parameters of interest (e.g.,
 648 sample size, trial count, effect size).
- 649 4. Summarise the simulated data to estimate likely power or precision of the research
 650 design options.

651 Ideally, in the above workflow, we would also fit a model to each dataset and
 652 summarise the model output, rather than the raw data. However, when each model takes
 653 several hours to build, and we may want to simulate many 1000s of datasets, it can be
 654 computationally demanding for desktop machines. So, for ease, here we just use the raw
 655 simulated datasets to guide future expectations.

656 In the below, we only provide a high-level summary of the process and let readers
 657 dive into the details within the tutorial should they feel so inclined.

658 **4.7.3 Fit a regression model and simulate one dataset.** We again use the
 659 data from Panis and Schmidt (2016) to provide a worked example. We fit an index coding
 660 model on a subset of timebins (six timebins in total) and for two prime conditions
 661 (congruent and incongruent). We chose to focus on a subsample of the data to ease the
 662 computational burden. We also used a full varying effects structure, with the model
 663 formula as follows:

```
event ~ 0 + timebin:prime + (0 + timebin:prime | pid)
```

664 We then took parameters from this model and used them to create a single dataset
 665 with 200 trials per condition for 10 individual participants. The raw data and the
 666 simulated data are plotted in Figure 12 and show quite close correspondence, which is
 667 re-assuring. But, this is only one dataset. What we really want to do is simulate many
 668 datasets and vary parameters of interest, which is what we turn to in the next section.

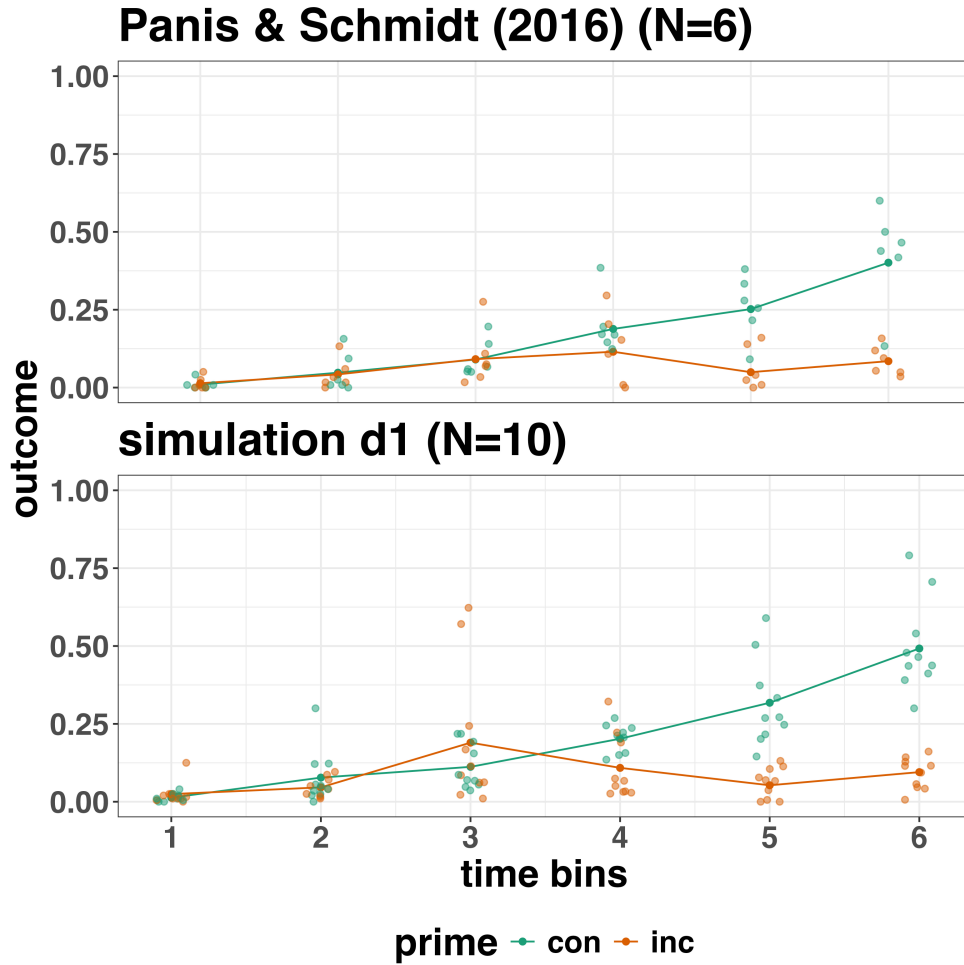


Figure 12. Raw data from Panis and Schmidt (2016) and simulated data from 10 participants.

669 4.7.4 Simulate and summarise data across a range of parameter values.

670 Here we use the same data simulation process as used above, but instead of simulating one
 671 dataset, we simulate 1000 datasets per variation in parameter values. Specifically, in
 672 Simulation 1, we vary the number of trials per condition (100, 200, and 400), as well as the
 673 effect size in bin 6. We focus on bin 6 only, in terms of varying the effect size, just to make
 674 things simpler and easier to understand. The effect size observed in bin 6 in this subsample
 675 of data was a 79% reduction in hazard value from the congruent prime (0.401 hazard
 676 value) to the incongruent prime condition (0.085 hazard value). In other words, a hazard

ratio of 0.21 (e.g., $0.085/0.401 = 0.21$). As a starting point, we chose three effect sizes, which covered a fairly broad range of hazard ratios (0.25, 0.5, 0.75), which correspond to a 75%, 50% and 25% reduction in hazard value as a function of prime condition.

Summary results from Simulation 1 are shown in Figure 13A. Figure 13A depicts statistical “power” as calculated by the percentage of lower-bound 95% confidence intervals that exclude zero when the difference between prime condition is calculated (congruent - incongruent). In other words, what fraction of the simulated datasets generated an effect of prime that excludes the criterion mark of zero. We are aware that “power” is not part of a Bayesian analytical workflow, but we choose to include it here, as it is familiar to most researchers in experimental psychology.

The results of Simulation 1 show that if we were targeting an effect size similar to the one reported in the original study, then testing 10 participants and collecting 100 trials per condition would be enough to provide over 95% power. However, we could not be as confident about smaller effects, such as a hazard ratio of 50% or 25%. From this simulation, we can see that somewhere between an effect size of a 50% and 75% reduction in hazard value, power increases to a range that most researchers would consider acceptable (i.e., >95% power). To probe this space a little further, we decided to run a second simulation, which varied different parameters.

In Simulation 2, we varied the effect size between a different range of values (0.5, 0.4, 0.3), which correspond to a 50%, 60% and 70% reduction in hazard value as a function of prime condition. In addition, we varied the number of participants per experiment between 10, 15, and 20 participants. Given that trial count per condition made little difference to power in Simulation 1, we fixed trial count at 200 trials per condition in Simulation 2. Summary results from Simulation 2 are shown in Figure 13B. A summary of these power calculations might be as follows (trial count = 200 per condition in all cases):

- For a 70% reduction (0.3 hazard ratio), N=10 would give nearly 100% power.

- 703 • For a 60% reduction (0.4 hazard ratio), N=10 would give nearly 90% power.
- 704 • For a 50% reduction (0.5 hazard ratio), N=15 would give over 80% power.

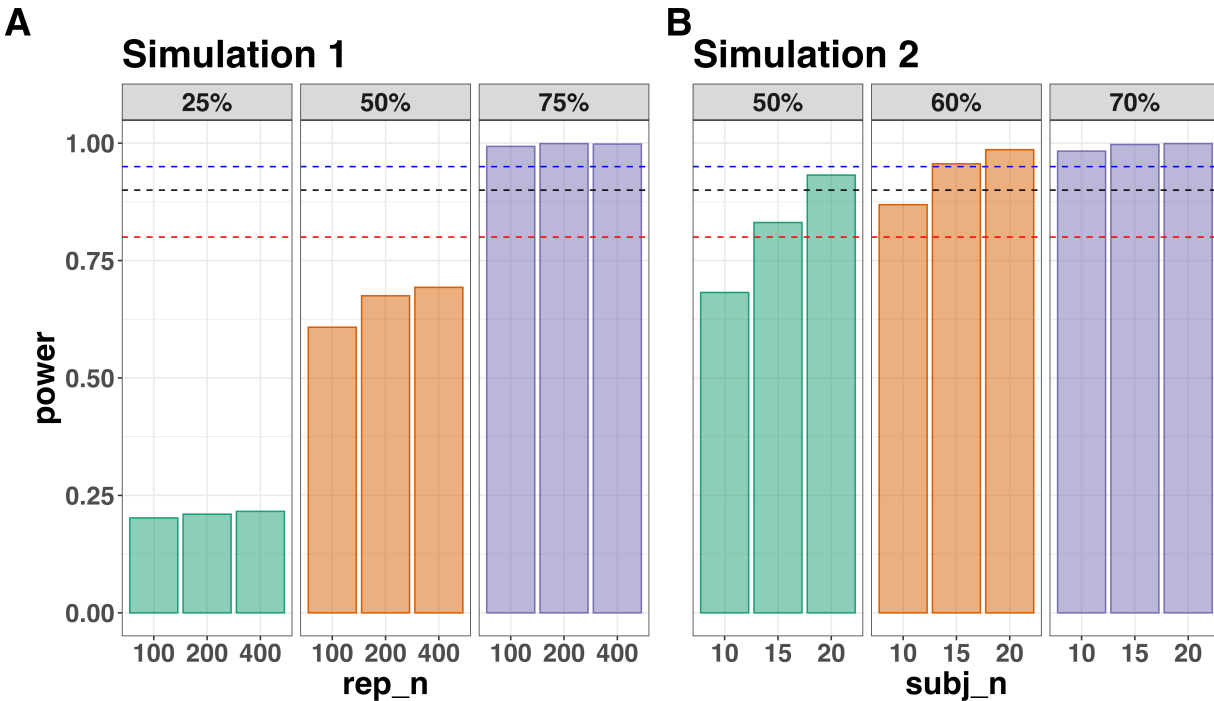


Figure 13. Statistical power across data Simulation 1 (A) and Simulation 2 (B). Power was calculated as the percentage of lower-bound 95% confidence intervals that exclude zero when the difference between prime condition is calculated (congruent - incongruent). In Simulation 1, the effect size was varied between a 25%, 50% and 75% reduction in hazard value, whereas the trial count was varied between 100, 200 and 400 trials per condition (the number of participants was fixed at N=10). In Simulation 2, the effect size was varied between a 50%, 60% and 70% reduction in hazard value, whereas the number of participants was varied between N=10, 15 and 20 (the number of trials per condition was fixed at 200). The dashed lines represent 80% (red), 90% (black) and 95% (blue) power. Abbreviations: rep_n = the number of trials per experimental condition; subj_n = the number of participants per simulated experiment.

705 **4.7.5 Planning decisions.** Now that we have summarised our simulated data,

706 what planning decisions could we make about a future study? More concretely, how many

707 trials per condition should we collect and how many participants should we test? Like

708 almost always when planning future studies, the answer depends on your objectives, as well

709 as the available resources (Lakens, 2022). There is no straightforward and clear-cut answer.

710 Some considerations might be as follows:

- 711 • How much power or precision are you looking to obtain in this particular study?

- 712 • Are you running multiple studies that have some form of replication built in?

- 713 • What level of resources do you have at your disposal, such as time, money and

714 personnel?

- 715 • How easy or difficult is it to obtain the specific type of sample?

716 If we were running this kind of study in our lab, what would we do? We might pick a

717 hazard ratio of 0.4 or 0.5 as a target effect size since this is much smaller than that

718 observed previously (Panis & Schmidt, 2016). Then we might pick the corresponding

719 combination of trial count per condition (e.g., 200) and participant sample size (e.g., N=10

720 or N=15) that takes you over the 80% power mark. If we wanted to maximise power based

721 on these simulations, and we had the time and resources available, then we would test

722 N=20 participants, which would provide >90% power for an effect size of 0.5.

723 **But**, and this is an important “but”, unless there are unavoidable reasons, no matter

724 what planning choices we made based on these data simulations, we would not solely rely

725 on data collected from one single study. Instead, we would run a follow-up experiment that

726 replicates and extends the initial result. By doing so, we would aim to avoid the Cult of

727 the Isolated Single Study (Nelder, 1999; Tong, 2019), and thus reduce the reliance on any

728 one type of planning tool, such as a power analysis. Then, we would look for common

729 patterns across two or more experiments, rather than trying to make the case that a single

730 study on its own has sufficient evidential value to hit some criterion mark.

731

5. Discussion

732 This main motivation for writing this paper is the observation that EHA and SAT
733 analysis remain under-used in psychological research. As a consequence, the field of
734 psychological research is not taking full advantage of the many benefits EHA/SAT provides
735 compared to more conventional analyses. By providing a freely available set of tutorials,
736 which provide step-by-step guidelines and ready-to-use R code, we hope that researchers
737 will feel more comfortable using EHA/SAT in the future. Indeed, we hope that our
738 tutorials may help to overcome a barrier to entry with EHA/SAT, which is that such
739 approaches require more analytical complexity compared to mean-average comparisons.
740 While we have focused here on within-subject, factorial, small- N designs, it is important to
741 realize that EHA/SAT can be applied to other designs as well (large- N designs with only
742 one measurement per subject, between-subject designs, etc.). As such, the general workflow
743 and associated code can be modified and applied more broadly to other contexts and
744 research questions. In the following, we discuss issues relating to model complexity and
745 interpretability, individual differences, as well as limitations of the approach and future
746 extensions.

747 **5.1 What are the main use-cases of EHA for understanding cognition and brain
748 function?**

749 For those researchers, like ourselves, who are primarily interested in understanding
750 human cognitive and brain systems, we consider two broadly-defined, main use-cases of
751 EHA. First, as we hope to have made clear by this point, EHA is one way to investigating
752 a “temporal states” approach to cognitive processes. EHA provides one way to uncover
753 when cognitive states may start and stop, as well as what they may be tied to or interact
754 with. Therefore, if your research questions concern **when** and **for how long** psychological
755 states occur, our EHA tutorials could be useful tools for you to use.

756 Second, even if you are not primarily interested in studying the temporal states of
757 cognition, EHA could still be a useful tool to consider using, in order to qualify inferences
758 that are being made based on mean-average comparisons. Given that distinctly different
759 inferences can be made from the same data based on whether one computes a
760 mean-average across trials or a RT distribution of events (Figure 1), it may be important
761 for researchers to supplement mean-average comparisons with EHA. One could envisage
762 scenarios where the implicit assumption of an effect manifesting across all of the time bins
763 measured would not be supported by EHA. Therefore, the conclusion of interest would not
764 apply to all responses, but instead it would be restricted to certain aspects of time.

765 5.2 Model complexity versus interpretability

766 EHA can quickly become very complex when adding more than one time scale, due to
767 the many possible higher-order interactions. For example, some of the models discussed in
768 Tutorial 2a, which we did not focus on in the main text, contain two time scales as
769 covariates: the passage of time on the within-trial time scale, and the passage of time on
770 the across-trial (or within-experiment) time scale. However, when trials are presented in
771 blocks, and blocks of trials within sessions, and when the experiment comprises three
772 sessions, then four time scales can be defined (within-trial, within-block, within-session,
773 and within-experiment). From a theoretical perspective, adding more than one time scale –
774 and their interactions – can be important to capture plasticity and other learning effects
775 that may play out on such longer time scales, and that are probably present in each
776 experiment in general. From a practical perspective, therefore, some choices need to be
777 made to balance the amount of data that is being collected per participant, condition and
778 across the varying timescales. As one example, if there are several timescales of relevance,
779 then it might be prudent for interpretational purposes to limit the number of experimental
780 predictor variables (conditions). This is of course where planning and data simulation
781 efforts would be important to provide a guide to experimental design choices (see Tutorial

782 4).

783 **5.3 Individual differences**

784 One important issue is that of possible individual differences in the overall location of
785 the distribution, and the time course of psychological effects. For example, when you wait
786 for a response of the participant on each trial, you allow the participant to have control
787 over the trial duration, and some participants might respond only when they are confident
788 that their emitted response will be correct. These issues can be avoided by introducing a
789 (relatively short) response deadline in each trial, e.g., 500 ms for simple detection tasks,
790 800 ms for more difficult discrimination tasks, or 2 s for tasks requiring extended high-level
791 processing. Because EHA can deal in a straightforward fashion with right-censored
792 observations (i.e., trials without an observed response in the analysis time window),
793 introducing a response deadline is recommended when designing RT experiments.
794 Furthermore, introducing a response deadline and asking participants to respond before the
795 deadline as much as possible, will also lead to individual distributions that overlap in time,
796 which is important when selecting a common analysis time window when fitting hazard
797 and conditional accuracy models.

798 But even when using a response deadline, participants can differ qualitatively in the
799 effects they display (see Panis, 2020). One way to deal with this is to describe and
800 interpret the different patterns. Another way is to run a clustering algorithm on the
801 individual hazard estimates across all bins and conditions. The obtained dendrogram can
802 then be used to identify a (hopefully big) cluster of participants that behave similarly, and
803 to identify a (hopefully small) cluster of participants with different behavioral patterns.
804 One might then exclude the smaller sub-group of participants before fitting a hazard model
805 or consider the possibility that different cognitive processes may be at play during task
806 performance across the different sub-groups.

807 Another approach to deal with individual differences is Bayesian prevalence (Ince,

808 Paton, Kay, & Schyns, 2021), which is a form of small- N approach (Smith & Little, 2018).

809 This method looks at effects within each individual in the study and asks how likely it

810 would be to see the same result if the experiment was repeated with a new person chosen

811 from the wider population at random. This approach allows one to quantify how typical or

812 uncommon an observed effect is in the population, and the uncertainty around this

813 estimate.

814 5.4 Limitations

815 Compared to the orthodox method – comparing mean-averages between conditions –

816 the most important limitation of multilevel hazard and conditional accuracy modeling is

817 that it might take a long time to estimate the parameters using Bayesian methods or the

818 model might have to be simplified significantly to use frequentist methods.

819 Another issue is that you need a relatively large number of trials per condition to

820 estimate the hazard function with high temporal resolution, which is required when testing

821 predictions of process models of cognition. Indeed, in general, there is a trade-off between

822 the number of trials per condition and the temporal resolution (i.e., bin width) of the

823 hazard function. Therefore, we recommend researchers to collect as many trials as possible

824 per experimental condition, given the available resources and considering the participant

825 experience (e.g., fatigue and boredom). For instance, if the maximum session length

826 deemed reasonable is between 1 and 2 hours, what is the maximum number of trials per

827 condition that you could reasonably collect? After consideration, it might be worth

828 conducting multiple testing sessions per participant and/or reducing the number of

829 experimental conditions. Finally, there is a user-friendly online tool for calculating

830 statistical power as a function of the number of trials as well as the number of participants,

831 and this might be worth consulting to guide the research design process (Baker et al., 2021).

We did not discuss continuous-time EHA, nor continuous-time SAT analysis. As indicated by Allison (2010), learning discrete-time EHA methods first will help in learning continuous-time methods. Given that RT is typically treated as a continuous variable, it is possible that continuous-time methods will ultimately prevail. However, they require much more data to estimate the continuous-time hazard (rate) function well. Thus, by trading a bit of temporal resolution for a lower number of trials, discrete-time methods seem ideal for dealing with typical psychological time-to-event data sets for which there are less than ~200 trials per condition per experiment.

5.5 Extensions

The hazard models in this tutorial assume that there is one event of interest. For RT data, this button-press event constitutes a single transition between an “idle” state and a “responded” state. However, in certain situations, more than one event of interest might exist. For example, in a medical or health-related context, an individual might transition back and forth between a “healthy” state and a “depressed” state, before being absorbed into a final “death” state. When you have data on the timing of these transitions, one can apply multi-state hazard models, which generalize EHA to transitions between three or more states (Steele, Goldstein, & Browne, 2004). Also, the predictor variables in this tutorial are time-invariant, i.e., their value did not change over the course of a trial. Thus, another extension is to include time-varying predictors, i.e., predictors whose value can change across the time bins within a trial (Allison, 2010). For example, when gaze position is tracked during a visual search trial, the gaze-target distance will vary during a trial when the eyes move around before a manual response is given; shorter gaze-target distances should be associated with a higher hazard of response occurrence. Note that the effect of a time-varying predictor (e.g., an occipital EEG signal) can itself vary over time.

856

6. Conclusions

857 Estimating the temporal distributions of RT and accuracy provide a rich source of
858 information on the time course of cognitive processing, which have been largely
859 undervalued in the history of experimental psychology and cognitive neuroscience. We hope
860 that by providing a set of hands-on, step-by-step tutorials, which come with custom-built
861 and freely available code, researchers will feel more comfortable embracing EHA and
862 investigating the temporal profile of cognitive states. On a broader level, we think that
863 wider adoption of such approaches will have a meaningful impact on the inferences drawn
864 from data, as well as the development of theories regarding the structure of cognition.

865

References

- 866 Allison, P. D. (1982). Discrete-Time Methods for the Analysis of Event Histories.
867 *Sociological Methodology*, 13, 61. <https://doi.org/10.2307/270718>
- 868 Allison, P. D. (2010). *Survival analysis using SAS: A practical guide* (2. ed). Cary, NC:
869 SAS Press.
- 870 Aust, F. (2019). *Citr: 'RStudio' add-in to insert markdown citations*. Retrieved from
871 <https://github.com/crsh/citr>
- 872 Aust, F., & Barth, M. (2023). *papaja: Prepare reproducible APA journal articles with R*
873 *Markdown*. Retrieved from <https://github.com/crsh/papaja>
- 874 Aust, F., & Barth, M. (2024). *papaja: Prepare reproducible APA journal articles with R*
875 *Markdown*. <https://doi.org/10.32614/CRAN.package.papaja>
- 876 Baker, D. H., Vilidaite, G., Lygo, F. A., Smith, A. K., Flack, T. R., Gouws, A. D., &
877 Andrews, T. J. (2021). Power contours: Optimising sample size and precision in
878 experimental psychology and human neuroscience. *Psychological Methods*, 26(3),
879 295–314. <https://doi.org/10.1037/met0000337>
- 880 Barr, D. J., Levy, R., Scheepers, C., & Tily, H. J. (2013). Random effects structure for
881 confirmatory hypothesis testing: Keep it maximal. *Journal of Memory and Language*,
882 68(3), 10.1016/j.jml.2012.11.001. <https://doi.org/10.1016/j.jml.2012.11.001>
- 883 Barth, M. (2023). *tinylabes: Lightweight variable labels*. Retrieved from
884 <https://cran.r-project.org/package=tinylabes>
- 885 Bates, D., Mächler, M., Bolker, B., & Walker, S. (2015). Fitting linear mixed-effects
886 models using lme4. *Journal of Statistical Software*, 67(1), 1–48.
887 <https://doi.org/10.18637/jss.v067.i01>
- 888 Bates, D., Maechler, M., & Jagan, M. (2024). *Matrix: Sparse and dense matrix classes and*
889 *methods*. Retrieved from <https://CRAN.R-project.org/package=Matrix>
- 890 Bengtsson, H. (2021). A unifying framework for parallel and distributed processing in r
891 using futures. *The R Journal*, 13(2), 208–227. <https://doi.org/10.32614/RJ-2021-048>

- 892 Blossfeld, H.-P., & Rohwer, G. (2002). *Techniques of event history modeling: New*
893 *approaches to causal analysis, 2nd ed* (pp. x, 310). Mahwah, NJ, US: Lawrence
894 Erlbaum Associates Publishers.
- 895 Box-Steffensmeier, J. M. (2004). Event history modeling: A guide for social scientists.
896 Cambridge: University Press.
- 897 Bürkner, P.-C. (2017). brms: An R package for Bayesian multilevel models using Stan.
898 *Journal of Statistical Software*, 80(1), 1–28. <https://doi.org/10.18637/jss.v080.i01>
- 899 Bürkner, P.-C. (2018). Advanced Bayesian multilevel modeling with the R package brms.
900 *The R Journal*, 10(1), 395–411. <https://doi.org/10.32614/RJ-2018-017>
- 901 Bürkner, P.-C. (2021). Bayesian item response modeling in R with brms and Stan. *Journal*
902 *of Statistical Software*, 100(5), 1–54. <https://doi.org/10.18637/jss.v100.i05>
- 903 DeBruine, L. M., & Barr, D. J. (2021). Understanding Mixed-Effects Models Through
904 Data Simulation. *Advances in Methods and Practices in Psychological Science*, 4(1),
905 2515245920965119. <https://doi.org/10.1177/2515245920965119>
- 906 Eddelbuettel, D., & Balamuta, J. J. (2018). Extending R with C++: A Brief Introduction
907 to Rcpp. *The American Statistician*, 72(1), 28–36.
908 <https://doi.org/10.1080/00031305.2017.1375990>
- 909 Eddelbuettel, D., & François, R. (2011). Rcpp: Seamless R and C++ integration. *Journal*
910 *of Statistical Software*, 40(8), 1–18. <https://doi.org/10.18637/jss.v040.i08>
- 911 Gabry, J., Češnovar, R., Johnson, A., & Broder, S. (2024). *Cmdstanr: R interface to*
912 *'CmdStan'*. Retrieved from <https://github.com/stan-dev/cmdstanr>
- 913 Gabry, J., Simpson, D., Vehtari, A., Betancourt, M., & Gelman, A. (2019). Visualization
914 in bayesian workflow. *J. R. Stat. Soc. A*, 182, 389–402.
915 <https://doi.org/10.1111/rssa.12378>
- 916 Gelman, A., Hill, J., & Vehtari, A. (2020). Regression and Other Stories.
917 <https://www.cambridge.org/highereducation/books/regression-and-other-stories/DD20DD6C9057118581076E54E40C372C>; Cambridge University Press.

- 919 https://doi.org/10.1017/9781139161879
- 920 Gelman, A., Vehtari, A., Simpson, D., Margossian, C. C., Carpenter, B., Yao, Y., ...
- 921 Modrák, M. (2020). *Bayesian Workflow*. arXiv.
- 922 https://doi.org/10.48550/arXiv.2011.01808
- 923 Girard, J. (2024). *Standist: What the package does (one line, title case)*. Retrieved from
- 924 https://github.com/jmgirard/standist
- 925 Grolemund, G., & Wickham, H. (2011). Dates and times made easy with lubridate.
- 926 *Journal of Statistical Software*, 40(3), 1–25. Retrieved from
- 927 https://www.jstatsoft.org/v40/i03/
- 928 Halley, E. (1693). VI. An estimate of the degrees of the mortality of mankind; drawn from
- 929 curious tables of the births and funerals at the city of breslaw; with an attempt to
- 930 ascertain the price of annuities upon lives. *Philosophical Transactions of the Royal*
- 931 *Society of London*, 17(196), 596–610. https://doi.org/10.1098/rstl.1693.0007
- 932 Heiss, A. (2021, November 10). A Guide to Correctly Calculating Posterior Predictions
- 933 and Average Marginal Effects with Multilevel Bayesian Models.
- 934 https://doi.org/10.59350/wbn93-edb02
- 935 Holden, J. G., Van Orden, G. C., & Turvey, M. T. (2009). Dispersion of response times
- 936 reveals cognitive dynamics. *Psychological Review*, 116(2), 318–342.
- 937 https://doi.org/10.1037/a0014849
- 938 Hosmer, D. W., Lemeshow, S., & May, S. (2011). *Applied Survival Analysis: Regression*
- 939 *Modeling of Time to Event Data* (2nd ed). Hoboken: John Wiley & Sons.
- 940 Ince, R. A., Paton, A. T., Kay, J. W., & Schyns, P. G. (2021). Bayesian inference of
- 941 population prevalence. *eLife*, 10, e62461. https://doi.org/10.7554/eLife.62461
- 942 Kantowitz, B. H., & Pachella, R. G. (2021). The Interpretation of Reaction Time in
- 943 Information-Processing Research 1. *Human Information Processing*, 41–82.
- 944 https://doi.org/10.4324/9781003176688-2
- 945 Kay, M. (2023). *tidybayes: Tidy data and geoms for Bayesian models*.

- 946 https://doi.org/10.5281/zenodo.1308151
- 947 Kelso, J. A. S., Dumas, G., & Tognoli, E. (2013). Outline of a general theory of behavior
948 and brain coordination. *Neural Networks: The Official Journal of the International*
949 *Neural Network Society*, 37, 120–131. https://doi.org/10.1016/j.neunet.2012.09.003
- 950 Kruschke, J. K., & Liddell, T. M. (2018). The Bayesian New Statistics: Hypothesis testing,
951 estimation, meta-analysis, and power analysis from a Bayesian perspective.
952 *Psychonomic Bulletin & Review*, 25(1), 178–206.
- 953 https://doi.org/10.3758/s13423-016-1221-4
- 954 Kurz, A. S. (2023a). *Applied longitudinal data analysis in brms and the tidyverse* (version
955 0.0.3). Retrieved from https://bookdown.org/content/4253/
- 956 Kurz, A. S. (2023b). *Statistical rethinking with brms, ggplot2, and the tidyverse: Second*
957 *edition* (version 0.4.0). Retrieved from https://bookdown.org/content/4857/
- 958 Lakens, D. (2022). Sample Size Justification. *Collabra: Psychology*, 8(1), 33267.
959 https://doi.org/10.1525/collabra.33267
- 960 Landes, J., Engelhardt, S. C., & Pelletier, F. (2020). An introduction to event history
961 analyses for ecologists. *Ecosphere*, 11(10), e03238. https://doi.org/10.1002/ecs2.3238
- 962 Luce, R. D. (1991). *Response times: Their role in inferring elementary mental organization*
963 (1. issued as paperback). Oxford: Univ. Press.
- 964 Makeham, W. M. (1860). *On the Law of Mortality and the Construction of Annuity Tables*.
965 The Assurance Magazine, and Journal of the Institute of Actuaries.
- 966 McElreath, R. (2020). *Statistical Rethinking: A Bayesian Course with Examples in R and*
967 *STAN* (2nd ed.). New York: Chapman and Hall/CRC.
- 968 https://doi.org/10.1201/9780429029608
- 969 Meyer, D. E., Osman, A. M., Irwin, D. E., & Yantis, S. (1988). Modern mental
970 chronometry. *Biological Psychology*, 26(1-3), 3–67.
971 https://doi.org/10.1016/0301-0511(88)90013-0
- 972 Müller, K., & Wickham, H. (2023). *Tibble: Simple data frames*. Retrieved from

- 973 https://CRAN.R-project.org/package=tibble
- 974 Nelder, J. A. (1999). From Statistics to Statistical Science. *Journal of the Royal Statistical Society. Series D (The Statistician)*, 48(2), 257–269. Retrieved from
975 https://www.jstor.org/stable/2681191
- 976
- 977 Neuwirth, E. (2022). *RColorBrewer: ColorBrewer palettes*. Retrieved from
978 https://CRAN.R-project.org/package=RColorBrewer
- 979 Panis, S. (2020). How can we learn what attention is? Response gating via multiple direct
980 routes kept in check by inhibitory control processes. *Open Psychology*, 2(1), 238–279.
981 https://doi.org/10.1515/psych-2020-0107
- 982 Panis, S., Moran, R., Wolkersdorfer, M. P., & Schmidt, T. (2020). Studying the dynamics
983 of visual search behavior using RT hazard and micro-level speed–accuracy tradeoff
984 functions: A role for recurrent object recognition and cognitive control processes.
985 *Attention, Perception, & Psychophysics*, 82(2), 689–714.
986 https://doi.org/10.3758/s13414-019-01897-z
- 987 Panis, S., Schmidt, F., Wolkersdorfer, M. P., & Schmidt, T. (2020). Analyzing Response
988 Times and Other Types of Time-to-Event Data Using Event History Analysis: A Tool
989 for Mental Chronometry and Cognitive Psychophysiology. *I-Perception*, 11(6),
990 2041669520978673. https://doi.org/10.1177/2041669520978673
- 991 Panis, S., & Schmidt, T. (2016). What Is Shaping RT and Accuracy Distributions? Active
992 and Selective Response Inhibition Causes the Negative Compatibility Effect. *Journal of
993 Cognitive Neuroscience*, 28(11), 1651–1671. https://doi.org/10.1162/jocn_a_00998
- 994 Panis, S., & Schmidt, T. (2022). When does “inhibition of return” occur in spatial cueing
995 tasks? Temporally disentangling multiple cue-triggered effects using response history
996 and conditional accuracy analyses. *Open Psychology*, 4(1), 84–114.
997 https://doi.org/10.1515/psych-2022-0005
- 998 Panis, S., Torfs, K., Gillebert, C. R., Wageman, J., & Humphreys, G. W. (2017).
999 Neuropsychological evidence for the temporal dynamics of category-specific naming.

- 1000 *Visual Cognition*, 25(1-3), 79–99. <https://doi.org/10.1080/13506285.2017.1330790>
- 1001 Panis, S., & Wagemans, J. (2009). Time-course contingencies in perceptual organization
1002 and identification of fragmented object outlines. *Journal of Experimental Psychology:
1003 Human Perception and Performance*, 35(3), 661–687.
1004 <https://doi.org/10.1037/a0013547>
- 1005 Pedersen, T. L. (2024). *Patchwork: The composer of plots*. Retrieved from
1006 <https://CRAN.R-project.org/package=patchwork>
- 1007 Pinheiro, J. C., & Bates, D. M. (2000). *Mixed-effects models in s and s-PLUS*. New York:
1008 Springer. <https://doi.org/10.1007/b98882>
- 1009 R Core Team. (2024). *R: A language and environment for statistical computing*. Vienna,
1010 Austria: R Foundation for Statistical Computing. Retrieved from
1011 <https://www.R-project.org/>
- 1012 Ripley, B., Venables, B., Bates, D. M., ca 1998), K. H. (partial. port, ca 1998), A. G.
1013 (partial. port, & polr), D. F. (support. functions for. (2024). *MASS: Support Functions
1014 and Datasets for Venables and Ripley's MASS*.
- 1015 Singer, J. D., & Willett, J. B. (2003). *Applied Longitudinal Data Analysis: Modeling
1016 Change and Event Occurrence*. Oxford, New York: Oxford University Press.
- 1017 Smith, P. L., & Little, D. R. (2018). Small is beautiful: In defense of the small-N design.
1018 *Psychonomic Bulletin & Review*, 25(6), 2083–2101.
1019 <https://doi.org/10.3758/s13423-018-1451-8>
- 1020 Steele, F., Goldstein, H., & Browne, W. (2004). A general multilevel multistate competing
1021 risks model for event history data, with an application to a study of contraceptive use
1022 dynamics. *Statistical Modelling*, 4(2), 145–159.
1023 <https://doi.org/10.1191/1471082X04st069oa>
- 1024 Teachman, J. D. (1983). Analyzing social processes: Life tables and proportional hazards
1025 models. *Social Science Research*, 12(3), 263–301.
1026 [https://doi.org/10.1016/0049-089X\(83\)90015-7](https://doi.org/10.1016/0049-089X(83)90015-7)

- 1027 Tong, C. (2019). Statistical Inference Enables Bad Science; Statistical Thinking Enables
1028 Good Science. *The American Statistician*, 73(sup1), 246–261.
1029 <https://doi.org/10.1080/00031305.2018.1518264>
- 1030 Townsend, J. T. (1990). Truth and consequences of ordinal differences in statistical
1031 distributions: Toward a theory of hierarchical inference. *Psychological Bulletin*, 108(3),
1032 551–567. <https://doi.org/10.1037/0033-2909.108.3.551>
- 1033 Wickelgren, W. A. (1977). Speed-accuracy tradeoff and information processing dynamics.
1034 *Acta Psychologica*, 41(1), 67–85. [https://doi.org/10.1016/0001-6918\(77\)90012-9](https://doi.org/10.1016/0001-6918(77)90012-9)
- 1035 Wickham, H. (2016). *ggplot2: Elegant graphics for data analysis*. Springer-Verlag New
1036 York. Retrieved from <https://ggplot2.tidyverse.org>
- 1037 Wickham, H. (2023a). *Forcats: Tools for working with categorical variables (factors)*.
1038 Retrieved from <https://forcats.tidyverse.org/>
- 1039 Wickham, H. (2023b). *Stringr: Simple, consistent wrappers for common string operations*.
1040 Retrieved from <https://stringr.tidyverse.org>
- 1041 Wickham, H., Averick, M., Bryan, J., Chang, W., McGowan, L. D., François, R., ...
1042 Yutani, H. (2019). Welcome to the tidyverse. *Journal of Open Source Software*, 4(43),
1043 1686. <https://doi.org/10.21105/joss.01686>
- 1044 Wickham, H., Çetinkaya-Rundel, M., & Grolemund, G. (2023). *R for data science: Import,
1045 tidy, transform, visualize, and model data* (2nd edition). Beijing Boston Farnham
1046 Sebastopol Tokyo: O'Reilly.
- 1047 Wickham, H., François, R., Henry, L., Müller, K., & Vaughan, D. (2023). *Dplyr: A
1048 grammar of data manipulation*. Retrieved from <https://dplyr.tidyverse.org>
- 1049 Wickham, H., & Henry, L. (2023). *Purrr: Functional programming tools*. Retrieved from
1050 [https://purrr.tidyverse.org/](https://purrr.tidyverse.org)
- 1051 Wickham, H., Hester, J., & Bryan, J. (2024). *Readr: Read rectangular text data*. Retrieved
1052 from <https://readr.tidyverse.org>
- 1053 Wickham, H., Vaughan, D., & Girlich, M. (2024). *Tidyr: Tidy messy data*. Retrieved from

- 1054 https://tidyverse.org
- 1055 Winter, B. (2019). *Statistics for Linguists: An Introduction Using R*. New York:
1056 Routledge. <https://doi.org/10.4324/9781315165547>
- 1057 Wolkersdorfer, M. P., Panis, S., & Schmidt, T. (2020). Temporal dynamics of sequential
1058 motor activation in a dual-prime paradigm: Insights from conditional accuracy and
1059 hazard functions. *Attention, Perception, & Psychophysics*, 82(5), 2581–2602.
1060 <https://doi.org/10.3758/s13414-020-02010-5>

1061

Supplementary material

1062 **A. Definitions of discrete-time hazard, survivor, probability mass, and**
 1063 **conditional accuracy functions**

1064 The shape of a distribution of waiting times can be described in multiple ways (Luce,
 1065 1991). After dividing time in discrete, contiguous time bins indexed by t , let RT be a
 1066 discrete random variable denoting the rank of the time bin in which a particular person's
 1067 response occurs in a particular experimental condition. Because waiting times can only
 1068 increase, discrete-time EHA focuses on the discrete-time hazard function

$$1069 \quad h(t) = P(RT = t | RT \geq t) \quad (1)$$

1070 and the discrete-time survivor function

$$1071 \quad S(t) = P(RT > t) = [1-h(t)].[1-h(t-1)].[1-h(t-2)] \dots [1-h(1)] \quad (2)$$

1072 and not on the probability mass function

$$1073 \quad P(t) = P(RT = t) = h(t).S(t-1) \quad (3)$$

1074 nor the cumulative distribution function

$$1075 \quad F(t) = P(RT \leq t) = 1-S(t) \quad (4)$$

1076 The discrete-time hazard function of event occurrence gives you for each bin the
 1077 probability that the event occurs (sometime) in that bin, given that the event has not
 1078 occurred yet in previous bins. This conditionality in the definition of hazard is what makes
 1079 the hazard function so diagnostic for studying event occurrence, as an event can physically
 1080 not occur when it has already occurred before. While the discrete-time hazard function
 1081 assesses the unique risk of event occurrence associated with each time bin, the
 1082 discrete-time survivor function cumulates the bin-by-bin risks of event *nonoccurrence* to
 1083 obtain the probability that the event occurs after bin t . The probability mass function
 1084 cumulates the risk of event occurrence in bin t with the risks of event nonoccurrence in

1085 bins 1 to $t-1$. From equation 3 we find that hazard in bin t is equal to $P(t)/S(t-1)$.

1086 For two-choice RT data, the discrete-time hazard function can be extended with the
 1087 discrete-time conditional accuracy function

$$1088 \quad ca(t) = P(\text{correct} \mid RT = t) \quad (5)$$

1089 which gives you for each bin the probability that a response is correct given that it is
 1090 emitted in time bin t (Allison, 2010; Kantowitz & Pachella, 2021; Wickelgren, 1977). The
 1091 $ca(t)$ function is also known as the micro-level speed-accuracy tradeoff (SAT) function.

1092 The survivor function provides a context for the hazard function, as $S(t-1) = P(RT >$
 1093 $t-1) = P(RT \geq t)$ tells you on how many percent of the trials the estimate $h(t) = P(RT =$
 1094 $t \mid RT \geq t)$ is based. The probability mass function provides a context for the conditional
 1095 accuracy function, as $P(t) = P(RT = t)$ tells you on how many percent of the trials the
 1096 estimate $ca(t) = P(\text{correct} \mid RT = t)$ is based.

1097 While psychological RT data is typically measured in small, continuous units (e.g.,
 1098 milliseconds), discrete-time EHA treats the RT data as interval-censored data, because it
 1099 only uses the information that the response occurred sometime in a particular bin of time
 1100 $(x,y]: x < RT \leq y$. If we want to use the exact event times, then we treat time as a
 1101 continuous variable, and let RT be a continuous random variable denoting a particular
 1102 person's response time in a particular experimental condition. Continuous-time EHA does
 1103 not focus on the cumulative distribution function $F(t) = P(RT \leq t)$ and its derivative, the
 1104 probability density function $f(t) = F(t)'$, but on the survivor function $S(t) = P(RT > t)$
 1105 and the hazard rate function $\lambda(t) = f(t)/S(t)$. The hazard rate function gives you the
 1106 instantaneous *rate* of event occurrence at time point t , given that the event has not
 1107 occurred yet.

1108 **B. Custom functions for descriptive discrete-time hazard analysis**

1109 We defined 12 custom functions that we list here.

- 1110 • censor(df,timeout,bin_width) : divide the time segment $(0, \text{timeout}]$ in bins, identify
1111 any right-censored observations, and determine the discrete RT (time bin rank)
- 1112 • ptb(df) : transform the person-trial data set to the person-trial-bin data set
- 1113 • setup_lt(ptb) : set up a life table for each level of 1 independent variable
- 1114 • setup_lt_2IV(ptb) : set up a life table for each combination of levels of 2
1115 independent variables
- 1116 • calc_ca(df) : estimate the conditinal accuracies when there is 1 independent variable
- 1117 • calc_ca_2IV(df) : estimate the conditional accuracies when there are 2 independent
1118 variables
- 1119 • join_lt_ca(df1,df2) : add the $\text{ca}(t)$ estimates to the life tables (1 independent
1120 variable)
- 1121 • join_lt_ca_2IV(df1, df2) : add the $\text{ca}(t)$ estimates to the life tables (2 independent
1122 variables)
- 1123 • extract_median(df) : estimate quantiles $S(t)._{50}$ (1 independent variable)
- 1124 • extract_median_2IV(df) : estimate quantiles $S(t)._{50}$ (2 independent variables)
- 1125 • plot_eha(df, subj, haz_yaxis=1, first_bin_shown=1, aggregated_data=F, Nsubj=6)
1126 : create plots of the discrete-time functions (1 independent variable), and specify the
1127 upper limit of the y-axis in the hazard plot, with which bin to start plotting, whether
1128 the data is aggregated across participants, and across how many participants
- 1129 • plot_eha_2IV(df, subj, haz_yaxis=1, first_bin_shown=1, aggregated_data=F,
1130 Nsubj=6) : create plots of the discrete-time functions (2 independent variables), and
1131 specify the upper limit of the y-axis in the hazard plot, with which bin to start
1132 plotting, whether the data is aggregated across participants, and across how many
1133 participants

1134 When you want to analyse simple RT data from a detection experiment with one
1135 independent variable, the functions calc_ca() and join_lt_ca() should not be used, and
1136 the code to plot the conditional accuracy functions should be removed from the function

₁₁₃₇ plot_eha(). When you want to analyse simple RT data from a detection experiment with
₁₁₃₈ two independent variables, the functions calc_ca_2IV() and join_lt_ca_2IV() should not
₁₁₃₉ be used, and the code to plot the conditional accuracy functions should be removed from
₁₁₄₀ the function plot_eha_2IV().

₁₁₄₁ **C. Link functions**

₁₁₄₂ Popular link functions include the logit link and the complementary log-log link, as
₁₁₄₃ shown in Figure 14.

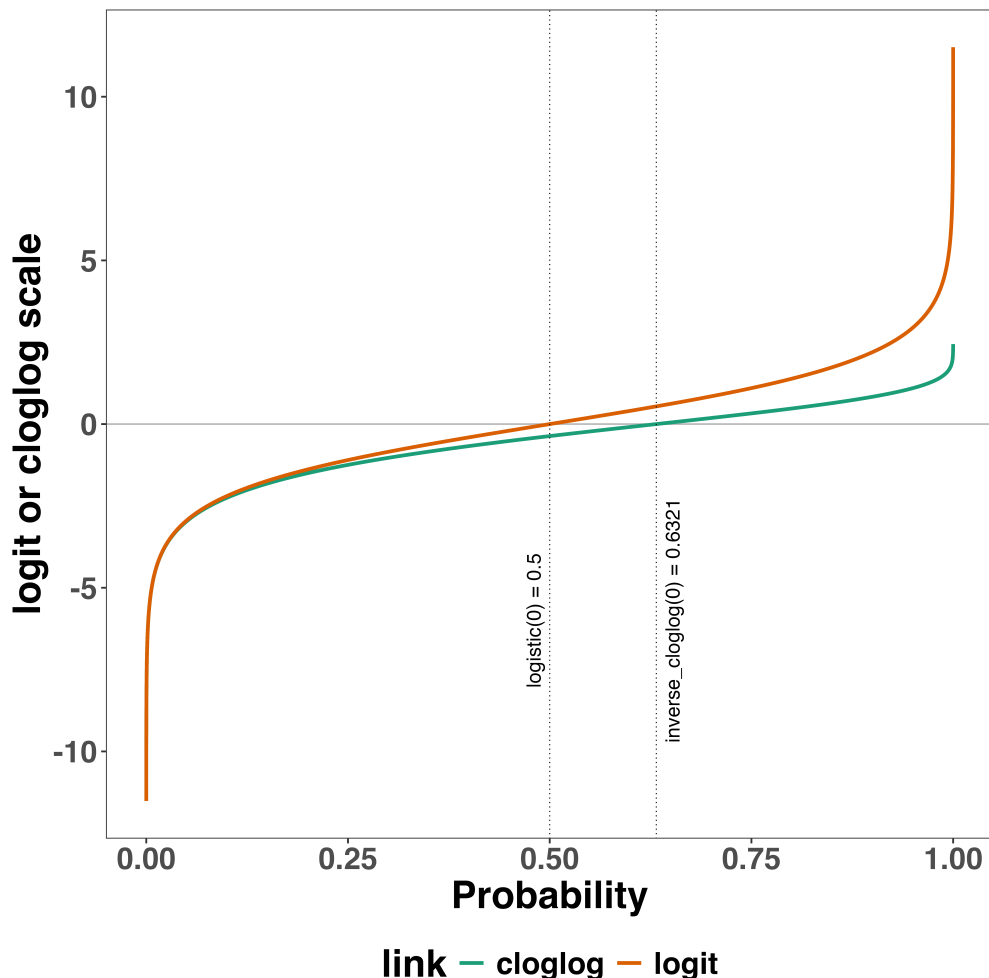


Figure 14. The logit and cloglog link functions.

₁₁₄₄ **D. Regression equations**

₁₁₄₅ An example (single-level) discrete-time hazard model with three predictors (TIME,
₁₁₄₆ X₁, X₂), the cloglog link function, and a second-order polynomial specification for TIME
₁₁₄₇ can be written as follows:

$$\begin{aligned} \text{cloglog}[h(t)] &= \ln(-\ln[1-h(t)]) = [\beta_0 \text{ONE} + \beta_1(\text{TIME}-9) + \beta_2(\text{TIME}-9)^2] + [\beta_3 X_1 + \beta_4 X_2 \\ &\quad + \beta_5 X_2(\text{TIME}-9)] \end{aligned} \quad (6)$$

₁₁₅₀ The main predictor variable TIME is the time bin index t that is centered on value 9
₁₁₅₁ in this example. The first set of terms within brackets, the parameters β_0 to β_2 multiplied
₁₁₅₂ by their polynomial specifications of (centered) time, represents the shape of the baseline
₁₁₅₃ cloglog-hazard function (i.e., when all predictors X_i take on a value of zero). The second
₁₁₅₄ set of terms (the beta parameters β_3 to β_5) represents the vertical shift in the baseline
₁₁₅₅ cloglog-hazard for a 1 unit increase in the respective predictor variable. Predictors can be
₁₁₅₆ discrete, continuous, and time-varying or time-invariant. For example, the effect of a 1 unit
₁₁₅₇ increase in X₁ is to vertically shift the whole baseline cloglog-hazard function by β_3
₁₁₅₈ cloglog-hazard units. However, if the predictor interacts linearly with TIME (see X₂ in the
₁₁₅₉ example), then the effect of a 1 unit increase in X₂ is to vertically shift the predicted
₁₁₆₀ cloglog-hazard in bin 9 by β_4 cloglog-hazard units (when TIME-9 = 0), in bin 10 by $\beta_4 +$
₁₁₆₁ β_5 cloglog-hazard units (when TIME-9 = 1), and so forth. To interpret the effects of a
₁₁₆₂ predictor, its β parameter is exponentiated, resulting in a hazard ratio (due to the use of
₁₁₆₃ the cloglog link). When using the logit link, exponentiating a β parameter results in an
₁₁₆₄ odds ratio.

₁₁₆₅ An example (single-level) discrete-time hazard model with a general specification for
₁₁₆₆ TIME (separate intercepts for each of six bins, where D1 to D6 are binary indicator
₁₁₆₇ variables identifying each bin) and a single predictor (X₁) can be written as follows:

$$\text{cloglog}[h(t)] = [\beta_0 D1 + \beta_1 D2 + \beta_2 D3 + \beta_3 D4 + \beta_4 D5 + \beta_5 D6] + [\beta_6 X_1] \quad (7)$$

₁₁₆₉ **E. Prior distributions**

₁₁₇₀ To gain a sense of what prior *logit* values would approximate a uniform distribution
₁₁₇₁ on the probability scale, Kurz (2023a) simulated a large number of draws from the
₁₁₇₂ Uniform(0,1) distribution, converted those draws to the log-odds metric, and fitted a
₁₁₇₃ Student's t distribution. Row C in Figure 15 shows that using a t-distribution with 7.61
₁₁₇₄ degrees of freedom and a scale parameter of 1.57 as a prior on the logit scale, approximates
₁₁₇₅ a uniform distribution on the probability scale. According to Kurz (2023a), such a prior
₁₁₇₆ might be a good prior for the intercept(s) in a logit-hazard model, while the N(0,1) prior in
₁₁₇₇ row D might be a good prior for the non-intercept parameters in a logit-hazard model, as it
₁₁₇₈ gently regularizes p towards .5 (i.e., a zero effect on the logit scale).

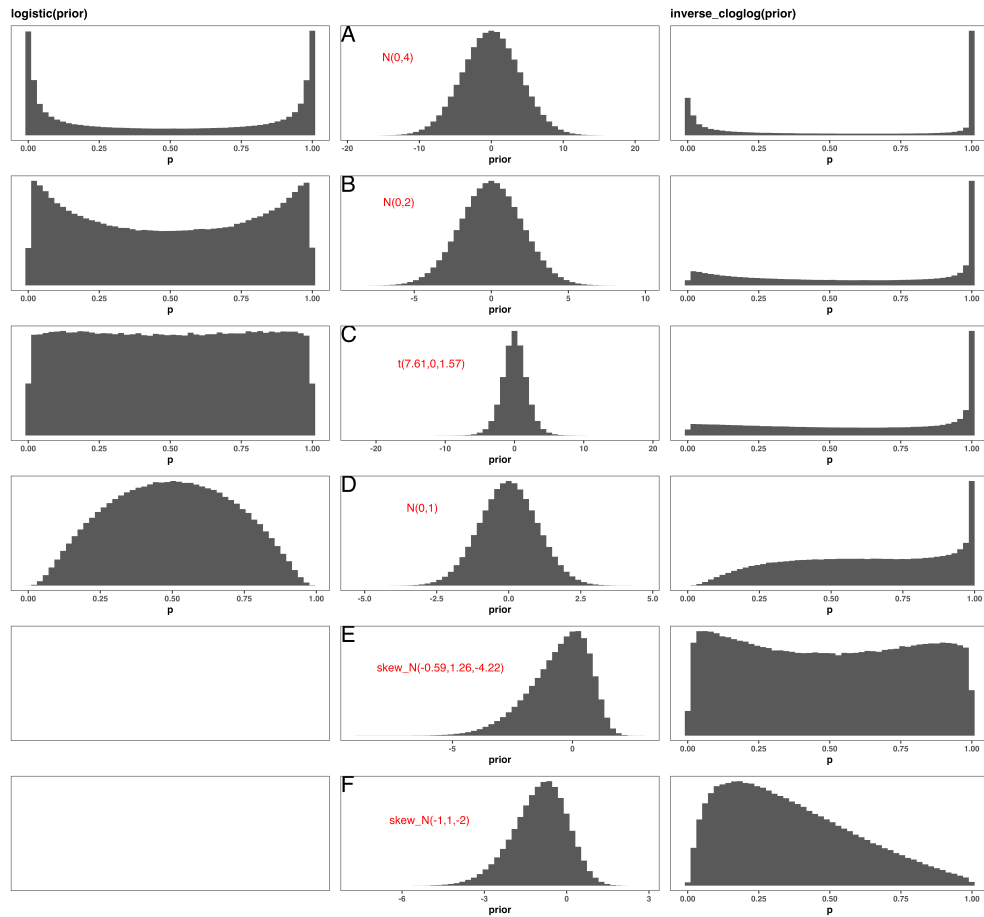


Figure 15. Prior distributions for the Intercept on the logit and/or cloglog scales (middle column), and their implications on the probability scale after applying the inverse-logit (or logistic) transformation (left column), and the inverse-cloglog transformation (right column).

1179 To gain a sense of what prior *cloglog* values would approximate a uniform distribution
 1180 on the hazard probability scale, we followed Kurz's approach and simulated a large number
 1181 of draws from the Uniform(0,1) distribution, converted them to the cloglog metric, and
 1182 fitted a skew-normal model (due to the asymmetry of the cloglog link function). Row E
 1183 shows that using a skew-normal distribution with a mean of -0.59, a standard deviation of
 1184 1.26, and a skewness of -4.22 as a prior on the cloglog scale, approximates a uniform
 1185 distribution on the probability scale. However, because hazard values below .5 are more
 1186 likely in RT studies, using a skew-normal distribution with a mean of -1, a standard

1187 deviation of 1, and a skewness of -2 as a prior on the cloglog scale (row F), might be a good
1188 weakly informative prior for the intercept(s) in a cloglog-hazard model.

1189 **F. Advantages of hazard analysis**

1190 Statisticians and mathematical psychologists recommend focusing on the hazard
1191 function when analyzing time-to-event data for various reasons. First, as discussed by
1192 Holden, Van Orden, and Turvey (2009), “probability density [and mass] functions can
1193 appear nearly identical, both statistically and to the naked eye, and yet are clearly different
1194 on the basis of their hazard functions (but not vice versa). Hazard functions are thus more
1195 diagnostic than density functions” (p. 331) when one is interested in studying the detailed
1196 shape of a RT distribution (see also Figure 1 in Panis, Schmidt, et al., 2020). Therefore,
1197 when the goal is to study how psychological effects change over time, hazard and
1198 conditional accuracy functions are the preferred ways to describe the RT + accuracy data.

1199 Second, because RT distributions may differ from one another in multiple ways,
1200 Townsend (1990) developed a dominance hierarchy of statistical differences between two
1201 arbitrary distributions A and B. For example, if $h_A(t) > h_B(t)$ for all t, then both hazard
1202 functions are said to show a complete ordering. Townsend (1990) concluded that stronger
1203 conclusions can be drawn from data when comparing the hazard functions using EHA. For
1204 example, when mean A < mean B, the hazard functions might show a complete ordering
1205 (i.e., for all t), a partial ordering (e.g., only for $t > 300$ ms, or only for $t < 500$ ms), or they
1206 may cross each other one or more times.

1207 Third, EHA does not discard right-censored observations when estimating hazard
1208 functions, that is, trials for which we do not observe a response during the data collection
1209 period in a trial so that we only know that the RT must be larger than some value (e.g.,
1210 the response deadline). This is important because although a few right-censored
1211 observations are inevitable in most RT tasks, a lot of right-censored observations are

1212 expected in experiments on masking, the attentional blink, and so forth. In other words, by
1213 using EHA you can analyze RT data from experiments that typically do not measure
1214 response times. As a result, EHA can also deal with long RTs in experiments without a
1215 response deadline, which are typically treated as outliers and are discarded before
1216 calculating a mean. This orthodox procedure leads to underestimation of the true mean.
1217 By introducing a fixed censoring time for all trials at the end of the analysis time window,
1218 trials with long RTs are not discarded but contribute to the risk set of each bin.

1219 Fourth, hazard modeling allows incorporating time-varying explanatory covariates
1220 such as heart rate, electroencephalogram (EEG) signal amplitude, gaze location, etc.
1221 (Allison, 2010). This is useful for linking physiological effects to behavioral effects when
1222 performing cognitive psychophysiology (Meyer et al., 1988).

1223 Finally, as explained by Kelso, Dumas, and Tognoli (2013), it is crucial to first have a
1224 precise description of the macroscopic behavior of a system (here: $h(t)$ and possibly $ca(t)$)
1225 functions) in order to know what to derive on the microscopic level. EHA can thus solve
1226 the problem of model mimicry, i.e., the fact that different computational models can often
1227 predict the same mean RTs as observed in the empirical data, but not necessarily the
1228 detailed shapes of the empirical RT hazard distributions. Also, fitting parametric functions
1229 or computational models to data without studying the shape of the empirical discrete-time
1230 $h(t)$ and $ca(t)$ functions can miss important features in the data (Panis, Moran, et al.,
1231 2020; Panis & Schmidt, 2016).